

MINISTRY OF EDUCATION AND SCIENCE OF THE REPUBLIC OF
KAZAKHSTAN



Institute of geology, petroleum and mining engineering

Department of Petroleum Engineering

Islam Karazhanov

The role of geomechanics in preventing wellbore instability

DIPLOMA PROJECT

Speciality 5B070800 – Petroleum Engineering

Almaty 2021

MINISTRY OF EDUCATION AND SCIENCE OF THE REPUBLIC OF
KAZAKHSTAN

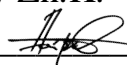


Institute of geology, petroleum and mining engineering

Department of Petroleum Engineering

APPROVED FOR DEFENSE

Head of the Petroleum
Engineering Department
Dairov Zh.K.



DIPLOMA PROJECT

Topic: «The role of geomechanics in preventing wellbore instability»

5B070800 – Petroleum Engineering

Performed by

Islam Karazhanov

Academic adviser
MSc in in Reservoir Evaluation
and Management

Baibussinova Zh. B.



Almaty 2021

Метаданные

Название:

The role of geomechanics in preventing wellbore instability

Автор:

Islam Karazhanov

Научный руководитель:

Zhanar Baibussinova

Подразделение:

ИГНИГД

Список возможных попыток манипуляций с текстом

В этом разделе вы найдете информацию, касающуюся манипуляций в тексте, с целью изменить результаты проверки. Для того, кто оценивает работу на бумажном носителе или в электронном формате, манипуляции могут быть невидимы (может быть также целенаправленное вписывание ошибок). Следует оценить, являются ли изменения преднамеренными или нет.

Замена букв		25
Интервалы		0
Микропробелы		0
Белые знаки		0
Парафразы (SmartMarks)		11

Объем найденных подоби

Обратите внимание! Высокие значения коэффициентов не означают плагиат. Отчет должен быть проанализирован экспертом.



25

Длина фразы для коэффициента подобия 2



7820

Количество слов



54708

Количество символов

Подобия по списку источников

Просмотрите список и проанализируйте, в особенности, те фрагменты, которые превышают КП №2 (выделенные жирным шрифтом). Используйте ссылку «Обозначить фрагмент» и обратите внимание на то, являются ли выделенные фрагменты повторяющимися короткими фразами, разбросанными в документе (совпадающие сходства), многочисленными короткими фразами расположенные рядом друг с другом (парафразирование) или обширными фрагментами без указания источника ("цитировать").

10 самых длинных фраз

Цвет текста

Порядковый номер	Название и адрес источника URL (название базы)	Количество идентичных слов (фрагментов)	Цвет текста
1	https://appssource.microsoft.com/en-us/product/power-bi-visuals/WA104380768	43	0.55 %
2	GEOMECHANICAL WELLBORE STABILITY MODELING OF EXPLORATORY WELLS - STUDY CASE AT MIDDLE MAGDALENA BASIN Alexander Rueda, Luz-Carime Valera Lara, Jenny-Mabel Carvajal Jiménez, Néstor-Fernando Saavedra Trujillo;	37	0.47 %
3	https://mountainscholar.org/handle/11124/170314	26	0.33 %
4	Designing an integrated production/distribution and inventory planning model of fixed-life perishable products Javad Rezaeian, keyvan Shokoufi, Iraj Mahdavi, Sepide Haghayegh;	17	0.22 %
5	Non-linear mass-spring system for large soft tissue deformations modeling	17	0.22 %

Sergei Nikolaev;

6	Modeling optimal long-term investment strategies of hybrid wind-thermal companies in restructured power market Mohammad Tolou ASKARI Mohd. Zainal Abdin Ab. KADIR Mehrdad TAHMASEBI Ehsan BOLANDIFAR;	15	0.19 %
7	Effects of different stress regimes on hydraulic fracture geometry: a particle flow code approach L. Duvillard;	14	0.18 %
8	GEOMECHANICAL WELLBORE STABILITY MODELING OF EXPLORATORY WELLS - STUDY CASE AT MIDDLE MAGDALENA BASIN Alexander Rueda, Luz-Carlme Valera Lara, Jenny-Mabel Carvajal Jiménez, Néstor-Fernando Saavedra Trujillo;	13	0.17 %
9	Multipoint boundary value problem for ordinary differential equations describing deformation of a three- layer beam Айсүлу Жумагалиева, Айжан Сіржебай, Сандуғаш Ескермес 5/23/2019 International IT University (математическое и компьютерное моделирование)	11	0.14 %
10	Multipoint boundary value problem for ordinary differential equations describing deformation of a three- layer beam Айсүлу Жумагалиева, Айжан Сіржебай, Сандуғаш Ескермес 5/23/2019 International IT University (Математическое и компьютерное моделирование)	11	0.14 %

из базы данных RefBooks (1.52 %)

ПОРЯДКОВЫЙ НОМЕР	НАЗВАНИЕ	КОЛИЧЕСТВО ИДЕНТИФНЫХ СЛОВ (ФРАГМЕНТОВ)	
Источник: Paperity			
1	GEOMECHANICAL WELLBORE STABILITY MODELING OF EXPLORATORY WELLS - STUDY CASE AT MIDDLE MAGDALENA BASIN Alexander Rueda, Luz-Carlme Valera Lara, Jenny-Mabel Carvajal Jiménez, Néstor-Fernando Saavedra Trujillo;	50 (2)	0.64 %
2	Designing an integrated production/distribution and inventory planning model of fixed-life perishable products Javad Rezaeian, keyvan Shokoufi, Iraj Mahdavi, Sepide Haghayegh;	17 (1)	0.22 %
3	Modeling optimal long-term investment strategies of hybrid wind-thermal companies in restructured power market Mohammad Tolou ASKARI Mohd. Zainal Abdin Ab. KADIR Mehrdad TAHMASEBI Ehsan BOLANDIFAR;	15 (1)	0.19 %

4	Effects of different stress regimes on hydraulic fracture geometry: a particle flow code approach L. Duvillard;	14 (1)	0.18 %
5	Pedestrian perception-based level-of-service model at signalized intersection crosswalks P. Vedagin, S. Marisamynathan;	6 (1)	0.08 %

Источник: <https://arxiv.org/>

1	Non-linear mass-spring system for large soft tissue deformations modeling Sergei Nikolaev;	17 (1)	0.22 %
---	--	--------	--------

из домашней базы данных (0.00 %)

ПОРЯДКОВЫЙ НОМЕР	НАЗВАНИЕ	КОЛИЧЕСТВО ИДЕНТИФНЫХ СЛОВ (ФРАГМЕНТОВ)
------------------	----------	---

из программы обмена базами данных (0.41 %) ■

ПОРЯДКОВЫЙ НОМЕР	НАЗВАНИЕ	КОЛИЧЕСТВО ИДЕНТИЧНЫХ СЛОВ (ФРАГМЕНТОВ)	
1	Multipoint boundary value problem for ordinary differential equations describing deformation of a three- layer beam Айсүлу Жумағалиева, Айжан Сіркебай, Сандуғаш Ескермес 5/23/2019 International IT University (Математическое и компьютерное моделирование)	32 (3)	0.41 %

из интернета (1.50 %) ■

ПОРЯДКОВЫЙ НОМЕР	ИСТОЧНИК URL	КОЛИЧЕСТВО ИДЕНТИЧНЫХ СЛОВ (ФРАГМЕНТОВ)	
1	https://appsource.microsoft.com/en-us/product/power-bi-visuals/WA104380768	43 (1)	0.55 %
2	https://mountainscholar.org/handle/11124/170314	37 (2)	0.47 %
3	http://www.reddiencia.cu/geobiblio/paper/2015_Ortiz%20GEF4-O2.pdf	17 (2)	0.22 %
4	https://pangea.stanford.edu/departments/geophysics/dropbox/STRESS/publications/MDZ%20PDF%27s/2006/2006_Empirical_relations_between_rock_strength.pdf	14 (2)	0.18 %
5	https://profiles.stanford.edu/mark-zoback?tab=research-and-scholarship	6 (1)	0.08 %

Список принятых фрагментов (нет принятых фрагментов)

ПОРЯДКОВЫЙ НОМЕР	СОДЕРЖАНИЕ	КОЛИЧЕСТВО ИДЕНТИЧНЫХ СЛОВ (ФРАГМЕНТОВ)
------------------	------------	---

MINISTRY OF EDUCATION AND SCIENCE OF THE REPUBLIC OF
KAZAKHSTAN



School of geology, petroleum and mining engineering

Department of Petroleum Engineering

CONFIRM

Head of the Petroleum
Engineering Department
Dairov Zh.K.

TASK

For completing the diploma project

For student Islam Karazhanov

Topic: “The role of geomechanics in preventing wellbore instability”

Approved by the order of university rector №2131-b from 24 November 2020

Deadline for completion the work: 18 May 2021

Initial data for the diploma project: in-situ stresses, well logging data, daily drilling reports.

Summary of the diploma project: Analysis will be based upon the background from field background research, the stress analysis and the sensitivity results.

The list of issues to be developed in the diploma project:

- a) Wellbore wall instability parameters;
- b) Geomechanical solution, oilfield planning;

Recommended main literature:

1. The geology of geomechanics: Petroleum geomechanical engineering in field development planning. (n.d.).
2. Bigoni, F. (2010). *OnePetro*. Retrieved from Karachaganak Field - Dynamic Data to drive geological modelling.
3. D., Z. M. (2006). *Empirical relations between rock strength and physical*. Retrieved from Journal of Petroleum Science and Engineering 5





SCHEDULE

for the diploma project preparation

Name of sections, list of issues being developed	Submission deadline to the Academic adviser	Notes
Introduction, methodology	15.02.2021	Task completed
Main part, database	02.03.2021	Task completed
Results	30.03.2021	Task completed
Conclusion	20.04.2021	Task completed

SIGNATURES

Of consultants and standard controller for the completed diploma project, indicating the relevant sections of the work (project).

The section titles	Consultant name (academic degree, title)	Date	Signature
Introduction, methodology	MSc, Baibussinova Zh. B.	15.02.2021	
Main part, database	MSc, Baibussinova Zh. B.	02.03.2021	
Results	MSc, Baibussinova Zh. B.	30.03.2021	
Normcontrol	MSc, Baibussinova Zh. B.	20.04.2021	

Academic Adviser



Baibussinova Zh.

The task was accepted by student:



Islam Karazhanov

Date

«18» May 2021

ANNOTATION

An impressive novelty in oil and gas production is the achievement of an oil reservoir layer without obstacles in the initial stages of drilling. Despite the initial problems, a geomechanical modeling process is required to achieve optimal drilling fluid pressure and also to drill safely in relation to pore pressure. The destruction of the borehole wall and other consequences during drilling are usually a mistake in the study of the stability of the borehole and the lack of an accurate forecast of pore pressure. The above reasons slow down the work at the drilling stage, which leads to additional finances.

In this thesis, work was done on geomechanical engineering, which is used at the initial stages of the development of oil fields. For a more correct study of the stability of the wellbore, the maximum width was used. Work has also been done with sensitivity analysis, which is used to test and evaluate each factor for changes in wellbore reliability. Many data were obtained from engineers working in the field, as due to the covid-19 pandemic and the moving of many employees to remote work, as well as the lack of access to practice for health safety. In addition, for a more accurate result, it was necessary to work with a specific depth, because many drilling reports indicate the general section of the wellbore. The sensitivity analysis was calculated in two methods, such as EXCEL and @RiskExcel. According to the results, among all the parameters: uniaxial compressive strength, Poisson's ratio, Young's modulus, the most effective is the maximum horizontal stress, since it acts perpendicular to the axis. According to this study, you can see the most common problems during drilling.

Key words: drilling, wellbore stability; sensitivity analysis; pore pressure, geomechanical modeling, in-situ stresses, covid-19, horizontal maximum stress, “Daily drilling reports”, uniaxial compressive strength, Poisson’s ratio, Young’s Modulus,

АННОТАЦИЯ

Внутренняя новизна в добыче нефти и газа это достижение нефтяного пласта без препятствий в начальных этапах бурения. Несмотря на первоначальных проблемах, для достижения оптимального давления бурового раствора и также для безопасного бурения по отношению к поровому давлению требуется процесс геомеханического моделирования. Разрушение стенки ствола скважины и также другие последствия при бурения как правило являются ошибкой при исследования стабильности ствола скважины и отсутствие точного прогноза порового давления. Вышеуказанные причины замедляют работу на этапе бурения, что приводит к дополнительному финансированию.

В данной дипломной статье была проделана работа по геомеханической инженерии, которую используют на начальных этапах разработки нефтяных месторождений. Для более правильного изучения устойчивости ствола скважины была использована максимальная ширина. Также была проделана работа с анализом чувствительности, который используется для проверки и оценки каждого фактора на изменения в надежности ствола скважины. Многие данные были получены от инженеров работающих в поле, так как в связи с пандемией коронавируса и переводом многих сотрудников на дистанционный режим работы, а также недопуском на практику для безопасности здоровья. Помимо этого, для более точного результата нужно было работать с конкретной глубиной, ведь во многих отчетов по бурению указывается общий участок ствола скважины. Анализ чувствительности был рассчитан двумя способами: EXCEL и @RiskExcel. Согласно результатам, среди всех параметров: прочность на одноосное сжатие, коэффициент Пуассона, модуль Юнга, наиболее эффективным является максимальное горизонтальное напряжение, так как оно действует перпендикулярно оси. Благодаря данной работе, можно увидеть наиболее часто встречающиеся проблемы во время бурения.

Ключевые слова: бурение, оптимальное давление, устойчивость ствола скважины; анализ чувствительности; геомеханическое моделирование, пандемия, отчет о бурении, максимальное горизонтальное напряжение, поровое давление, смещение стенки, , прочность на одноосное сжатие, коэффициент Пуассона, модуль Юнга, измерение диаметра скважины.

АҢДАТПА

Мұнай мен газ өндірудегі әсерлі жаңалық-бұрғылаудың бастапқы кезеңдерінде кедергісіз мұнай қабатына қол жеткізу. Бастапқы проблемаларға қарамастан, бұрғылау ерітіндісінің оңтайлы қысымына қол жеткізу және біркелкі қысымға қатысты қауіпсіз бұрғылау геомеханикалық модельдеу процесін қажет етеді. Ұңғыманың қабырғасының бұзылуы және бұрғылау кезіндегі басқа да салдарлар, әдетте, ұңғыманың тұрақтылығын зерттеудегі қателік болып табылады және кеуек қысымының нақты болжамының болмауы. Жоғарыда аталған себептер бұрғылау кезеңіндегі жұмысты баяулатады, бұл қосымша қаржыландыруға әкеледі.

Бұл дипломдық мақалада мұнай кен орындарын игерудің бастапқы кезеңдерінде қолданылатын геомеханикалық инженерия бойынша жұмыс жасалды. Ұңғыманың тұрақтылығын дұрыс зерттеу үшін максималды ені қолданылды. Сондай-ақ, ұңғыманың сенімділігіндегі өзгерістерді тексеру және бағалау үшін қолданылатын сезімталдықты талдаумен жұмыс жасалды. Көптеген мәліметтер далада жұмыс істейтін инженерлерден алынды, өйткені коронавирус пандемиясына және көптеген қызметкерлерді қашықтықтан жұмыс режиміне ауыстыруға, сондай-ақ денсаулық қауіпсіздігі үшін практикаға жіберілмеуіне байланысты. Сонымен қатар, дәлірек нәтиже алу үшін белгілі бір тереңдікпен жұмыс істеу керек болды, өйткені бұрғылау туралы көптеген есептер ұңғыманың жалпы ауданын көрсетеді. Сезімталдықты талдау екі жолмен есептелді: EXCEL және @riskexcel. Нәтижелерге сәйкес, барлық параметрлердің ішінде: бір осьтік сығымдау күші, Пуассон коэффициенті, Юнг модулі, ең тиімдісі-максималды көлденең кернеу, өйткені ол оське перпендикуляр әрекет етеді. Осы жұмыстың арқасында бұрғылау кезінде жиі кездесетін мәселелерді көруге болады

Түйінді сөздер: бұрғылау, оңтайлы қысым, ұңғыманың тұрақтылығы; сезімталдықты талдау; геомеханикалық модельдеу, пандемия, бұрғылау туралы есеп, максималды көлденең кернеу, кеуек қысымы, қабырғаның жылжуы, бір осьтік сығымдау күші, Пуассон коэффициенті, Юнг модулі,

TABLE OF CONTENT

INTRODUCTION	15
1.1 Wellbore instability	15
1.2 Objectives of the study	15
1.3 Available data	16
Problem diagnostic	17
2.1 Problem diagnostic methodology	17
2.2 Stress Analysis	18
2.3 Sensitivity Analyses	19
2.4 Results and Recommendations	20
MAIN PART	20
3.2 Well X-77 description	20
3.3 Well X-77 Geomechanical Interpretation	23
Database	27
a. Stresses and Pore Pressure	28
b. Initial input data	28
RESULTS	33
6.1.1 Offset Well Behaviour	33
6.1.2 Sensitivity analysis	33
CONCLUSIONS AND RECOMMENDATION	39
7.1 Conclusion	39
Glossary	41
REFERENCES	45
Appendix A	46
Appendix B	54

List of figures:

<u>Figure 1- The Leak-Off Test (LOT), Formation Integrity Test (FIT) values and minimum horizontal stress (σ_{Hmin}) TVDbgl (True Vertical Depth below ground level) trend</u>	16
<u>Figure 2- Relief plot illustrating the tangential (or ‘hoop’) stress distribution around a vertical borehole in an anisotropic stress field.</u>	18
<u>Figure 3-Faulting regimes</u>	19
<u>Figure 4-Well X-88- 16” Section Time Summary</u>	22
<u>Figure 5-Well X-88- 12 1/4” Section Time Summary</u>	22
<u>Figure 6-Well X-88- 12 1/4” Section Time Summary Continued</u>	23
<u>Figure 7-Well X-88- 8 1/2” Section Time Summary</u>	23
<u>Figure 8- Model Prediction and Caliper Comparison for Well X-88.....</u>	25
<u>Figure 9-CBIL Log Showing Breakout in the Upper Serpukhovian of Well X-88 (4709 – 4714.8 m MD).....</u>	26
<u>Figure 10-The LOT, FIT values and SHmin TVDbgl trend</u>	28
<u>Figure 11-- Sensitivity analysis of in-situ stresses and pressures effect on wellbore stability.</u>	35
<u>Figure 12-Sensitivity analysis of geomechanical factors on wellbore stability.....</u>	36
<u>Figure 13-Probability of breakout pressure.....</u>	37
<u>Figure 14- Contribution of various input parameters to minimum pressure to prevent breakouts.....</u>	38

List of tables:

<u>Table 1-lithology, density of X-88 well</u>	27
<u>Table 2- True vertical depth (TVD), vertical stress (σ_v), maximum and minimum horizontal stresses (σ_{Hmax} , σ_{hmin}) values.</u>	29
<u>Table 3- Empirical relationships between UCS and other physical properties in sandstones</u>	30
<u>Table 4-Empirical relationships between UCS and other physical properties in sandstones.</u>	31
<u>Table 5-Young's Modulus for different formations.</u>	31
<u>Table 6-Statistical relationships for estimation of modulus of elasticity for different geologic formations and all formations together</u>	32
<u>Table 7-Input data ranges for the wellbore-stability sensitivity analysis</u>	36

INTRODUCTION

1.1 Wellbore instability

Wellbore instability problems bring significant cost increases to drilling operations. These problems can occur in a variety of forms including stuck pipe, loss circulation, hole enlargement, unintentionally induced tensile fractures or difficult directional control incidents. In severe conditions, wellbore instability can increase non-productive time and create simultaneous occurrences of multiple instability incidents, which potentially can lead to losing the well if they are not handled with proper mitigation. Wellbore instability is a function of imbalance in the required wellbore pressure applied and the fluid pressure in the formation, in addition to chemical interactions between the formation and the drilling or completion fluids, and interactions between these fluids and native formation fluid. Deviation and azimuth of the well also influence the wellbore stability as the stress distribution around the wellbore is dependent on the orientation of the wellbore, with respect to the in-situ stresses and the hoop stresses introduced through drilling the wellbore. To avoid wellbore instability problems in drilling, a proper well design needs to be developed for the formations to be drilled and completed for production, which requires understanding of the in-situ stress state, pore pressure, and geomechanical properties of the reservoir formation.

1.2 Objectives of the study

Wellbore instability problems significantly increase the cost of drilling and operations in the petroleum engineering companies. At the initial stages of drilling and completion, the main object are to predict the stability of the wellbore during construction and maintain integrity during its production.

The main targets of the study were to:

- Measure the proportion of each parameter effect on the stability of a wellbore.
- Develop a calibrated geomechanical model for each area of the field aligned with the pore pressure, fracture gradient and in situ stress profiles
- Advise mud properties and practices, Rate Of Penetrations (ROP)s, swab and surge allowances, torque and drag monitoring etc. that are required to minimize potential drilling issues.
- Study the effect of stress direction on instability and highlight any changes due to borehole deviation

1.3 Available data

The data availability is one of the invocation faced during the work. Geomechanical engineering was considered as an main part, but values needed for calculations were limited by a specific depth (0-5100m).

Well Logging Data

Wireline logs are one of source of geomechanical characterization in this research study. The log data are used to determine the compressive failure within the field and this is well-illustrated by numerous image and dual-caliper logs.

Daily Drilling Reports

From this reports, drilling progress chart has been created showing many challenges that caused non-productive time (NPT) during drilling. This data is useful to determine the main cause of wellbore instabilities.

In-situ stresses

The processed Formation Integrity Test (FIT) and Leakoff Test (LOT) results as in-situ stresses were part of the data reviewed for this study by the company representatives. The dataset for the X Field is limited.

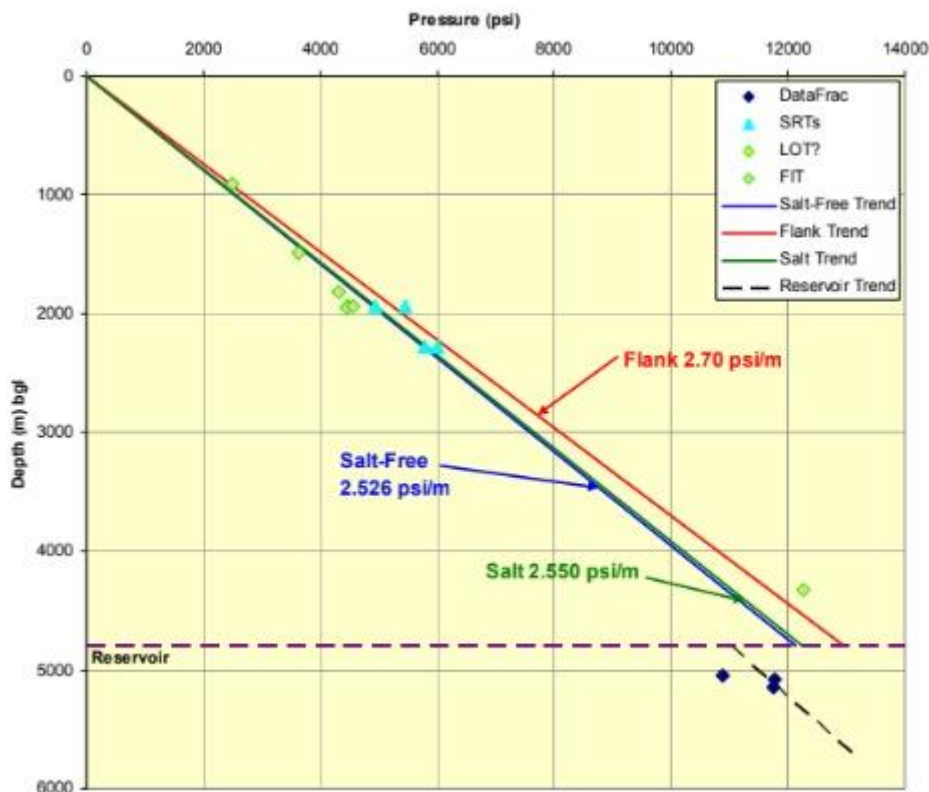


Figure 1- The Leak-Off Test (LOT), Formation Integrity Test (FIT) values and minimum horizontal stress (σ_{Hmin})

Problem diagnostic

2.1 Problem diagnostic methodology

Geomechanical research depends on the relation between mechanical properties and qualities of rocks with the stresses acting on the site. At the moment when the stresses acting in the rock are below the yield strength, the rocks act flexibly and the deformations are small. However, if the stress changes resulting from excavation during drilling, or from pore failure or thermal changes, exceed the compressive yield strength, peak strength, or pore fracture strength, the rock will explode as a result of shear or compaction, causing indirect irreversible deformation. The land articulation of the geomechanical, or basic, forms that are liable for the improvement of numerous oilfields incorporate collapsing, blaming, breaking and diapirism. The stress regimes and strains going with these deformations can control the current day initial stresses and surfaces in numerous reservoirs. **[Error! Reference source not found.]**

The mechanical stability of a well depends on the effective stresses in place, the mechanical strength of the exposed layers, and the geometry of the well. The occurrence of instability of the holes, as a rule, is the result of mechanical and chemical influences. Mechanical instability occurs when the stresses in the wellbore exceed the mechanical strength of the formation, either in tension (which leads to formation failure) or in compression (which leads to breakouts, collapse, or collapse of the formation). The onset of formation failure (or tensile failure) indicates drilling with too high a mud weight, and a borehole breakout suggests that the mud weight is too low. Between these two extremes is the range of drilling mud weights for safely drilling a well - the safe drilling window. The upper limit of this window is controlled under certain circumstances by the minimum horizontal stress, when it can be expected that the ECDs (Effective Circulation Density) above the minimum EMW (Effective Mud Mass) for the well section can lead to losses due to the opening of previously existing unfavorably oriented natural cracks.

The methodology is based on an incremental design approach, and the quality of forecasts depends on the accuracy, variability, and quantity of field data. It is therefore essential to conduct assessments as new field information becomes available. This would increase the credibility of the assessment.

The methodology used for this study was divided into five main research areas: problem diagnosis, stress analysis, sensitivity analysis, and finally, results and recommendations.

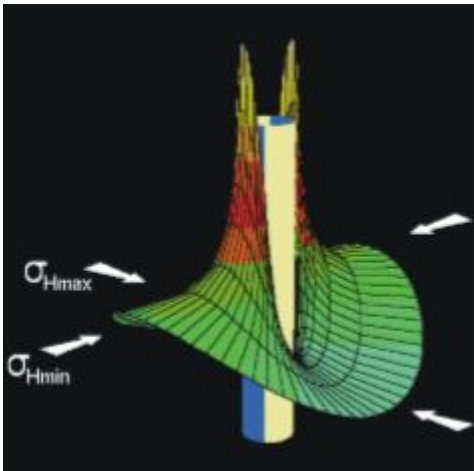


Figure 2- Relief plot illustrating the tangential stress distribution around a vertical borehole in an anisotropic stress field. The coincidence of regions of highest and least tangential stress with the azimuths of σ_{Hmin} and σ_{Hmax} respectively.

The figure above shows a graphical representation of the values of tangential (or "ring") stresses around the wall. Two water zones with high compressive stresses will correspond to the breakout areas if the stresses exceed the rock strength. They are always aligned in the direction of the lowest stress in the vertical wells. Areas of low tangential stresses are aligned in the direction of maximum stresses and areas of tensile stresses.

2.2 Stress Analysis

Stress is defined as the force acting on a unit area that pushes or pulls a body of material. The magnitude of the force and the properties of the material determine the reaction of the material to the applied stress. Zobak (2010) describes the stress as a second-rank tensor with nine components that determine the density of forces acting on all surfaces passing through a given point. All these nine components are shown as:

$$S = \begin{bmatrix} S_{11} & S_{12} & S_{13} \\ S_{21} & S_{22} & S_{23} \\ S_{31} & S_{32} & S_{33} \end{bmatrix},$$

The nine components define the direction the force and the face it is acting on. Since each component is acting perpendicular to two axis and acting in one direction, there are nine magnitudes and three directions to define.

As shown in Figure below vertical stress prevails in the normal fault mode; fault slip occurs when the minimum horizontal stress reaches a relatively lower value than the vertical stress and pore pressure. When there is a significant difference between the maximum horizontal stress and the minimum horizontal stress, a slip error will be created. On the other hand, the reverse fault is caused by a large difference between

the maximum horizontal voltage and the vertical voltage. As soon as both horizontal stresses exceed the vertical ones, the earth's crust shortens.

Table 1- Definition of S1 and S3 for Andersonian faulting classifications (PetroWiki, 2015) [Error! Reference source not found.]

Fault Regime	S_1	S_3
Normal	S_v	S_{Hmin}
Strike-slip	S_{Hmax}	S_{Hmin}
Reverse	S_{Hmax}	S_v

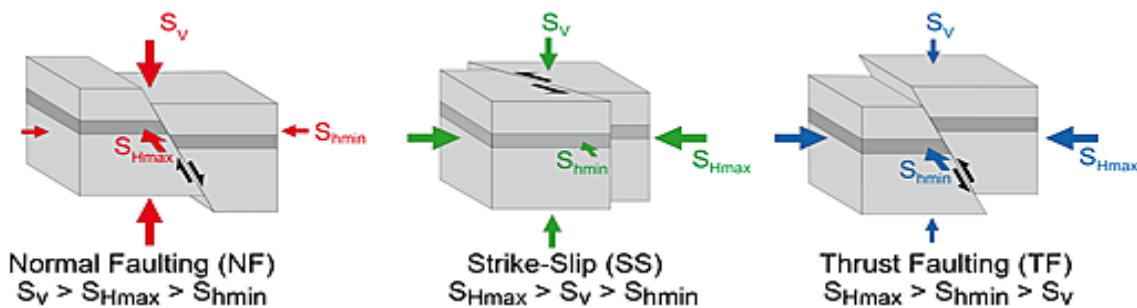


Figure 3-Faulting regimes [Error! Reference source not found.] (Ahangari, 2017)

The X field was interpreted as having a Strike-slip mode. Consequently, the stress difference is highest for a vertical well compared to horizontal wells. The well pressure required to prevent a breakout is highest in vertical wells and usually decreases with increasing slope. However, for wells with a high slope, there is a strong azimuthal dependence. It may not be possible to use sufficiently high mud weights to prevent failure, and some breakthroughs must be allowed. Breakouts have generally been tolerated recently in high-slope wells due to problems with well cleaning and steering. The mud weight may not be able to be reduced in high inclination wells compared with vertical wells for these reasons. However, it may be possible to maintain the mud weight in use in the vertical wells through the overburden should more challenging well designs be proposed.

2.3 Sensitivity Analyses

Sensitivity analysis is a method for evaluating the constantability of a system. The sensitivity of each factor was developed by changing its meanings in a given values while keeping all other factors constant at their base value. Then there were created graphs, according to the equations that we found and these adjusted equations are

used to quantify the sensitivity of each factor. The sensitivity of displacement of the borehole walls is a criterion of stability to the factors of these types of rocks.

Also for more accurate results, we performed another sensitivity analysis. Sensitivity analysis was conducted with the @RISK Excel, a program that provided calculation of the risk severity using Monte Carlo simulations to show probabilities of specific input parameters.

2.4 Results and Recommendations

The final portion of this report will be the examination of results. Analysis will be based upon the findings from field background research, previous work, the stress analysis and the sensitivity results. Relationships between the stress anisotropy, acoustic properties and petrophysical properties will be discussed in an attempt to aid in optimization of the future drilling and completion designs. The analysis portion of the report will also provide recommendations for future work.

MAIN PART

3.2 Well X-77 description

The 16” section

The 16” section was drilled vertically with water-based mud (WBM), with mud weight increasing gradually from 1.25 SG at the start of the section to 1.40 SG once TD was reached at 1956 m MD. A drilling time summary of the 16” section is presented in Figure 4. Minor light spots were found on several short wiper trips in the Jurassic and Triassic periods, and some expansion was required. Some more stable bottlenecks, requiring both read and reverse flow, have been tested to the base of the Triassic. Small glasses, with rats of the order of 3.6 m³ / h, were also tested after drying in the upper Triassic. One logging run was carried out successfully (DLL-MLL-MAC-DSL) and the 13 ³/₈” casing was run to TD twelve days after the section was started.

The 12 1/4” section

The 12 ¹/₄” section of Well X-88 took 67 days to complete and for this reason it is presented on two drilling time summaries shown in Figure 5 and Figure 6. Losses were experienced throughout the section, although maximum rates of only 2 m³/hr were recorded. The drilling mud weight of 1.40 – 1.41 SG was used for drilling up to

the middle of Tartary, where the drilling mud density was increased to 1.48 SG. The site was drilled vertically to a depth of 4,674 m in the upper part of the Artinskoye after very slow drilling through the Irenskaya and Filippovskaya formations. Frequent bottlenecks, caverns, and the need for sweep and reverse sweep were observed at the base of the Triassic and in the upper part of Tartary, although these problems decreased in frequency after the mud weight was increased from 1.41 to 1.48 s. Some bottlenecks and packages were also observed in the Irena formation. The frequent trips carried out in the second half of the section were mostly trouble-free, and three logging runs (DLL-MLL-DSL-MAC; ZDEN-CN-GR; STAR-CBIL-GR) were carried out with some overpulls noted.

The 8 1/2" section

The 8 1/2" section was drilled with a mud weight of 1.18 SG (WBM) and was drilled vertically to a TD of 5275 m MD (cored from 5005 – 5188 m MD) with a maximum loss rate of 0.5 m³/hr. No problems were experienced while drilling, coring and during the multiple trips, and three logging runs were carried out successfully (DLL-MLL-DSL-MAC; ZDL-CN-DSL; STAR-CBIL-GR). On the fourth logging run the RCI tool became stuck in the Upper Serpukhovian and the cable was cut. Fishing operations were successful and the RCI log was re-run, followed by the MRIL logging string. The section was plugged and sidetracked.

The X-88 STH well was launched in the 8 1/2 " well from a depth of 4986 m in the Lower Serpukhov and was built horizontally in the north-west azimuth. A brief description of the drilling time, showing both 8 sections 1/2" and 57/8", is shown in Figure 5.

The short section was drilled from 4,986 m to 5,182 m in an 8 1/2-inch hole prior to launching the 7-inch liner. In this section, there were no obvious problems with the drilling mud mass (WBM) of 1.19 SG and the maximum loss rate of 1 m³/hour. The well was then continued in a 5 7 × 8 inch well and drilled to TD 5716 m MD in seven days using a drilling mud weight (WBM) of 1.08 SG. One trip was required due to a MWD tool failure, the chisel was marked as "rolled", and the string was found to be hanging while the slide was being drilled. However, no further problems occurred, and two runs of drill pipes (DL-ML-MEC-DSL-TERM; ZDL-ZDEN-CN) were successfully conducted in the open well.

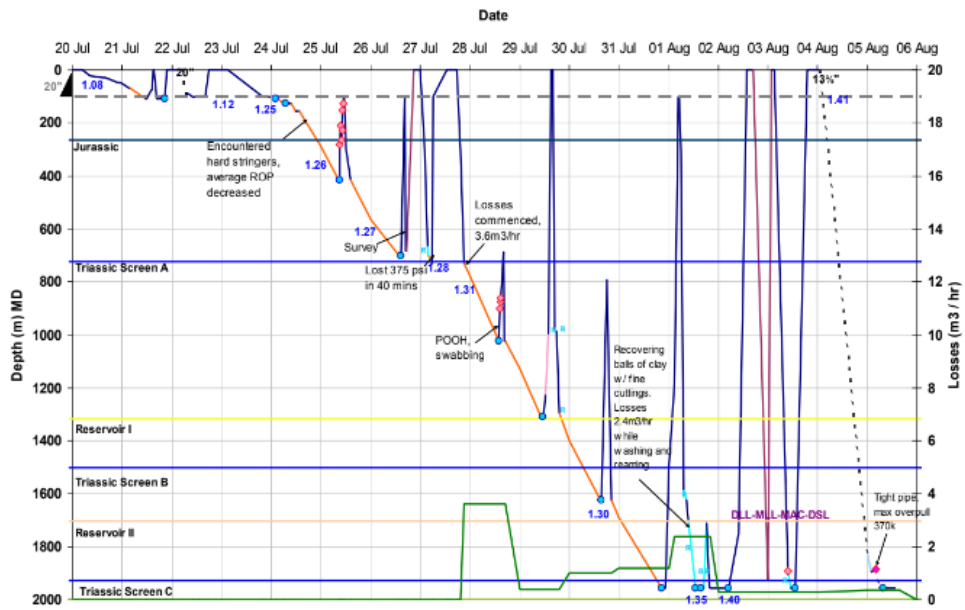


Figure 4-Well X-88- 16" Section

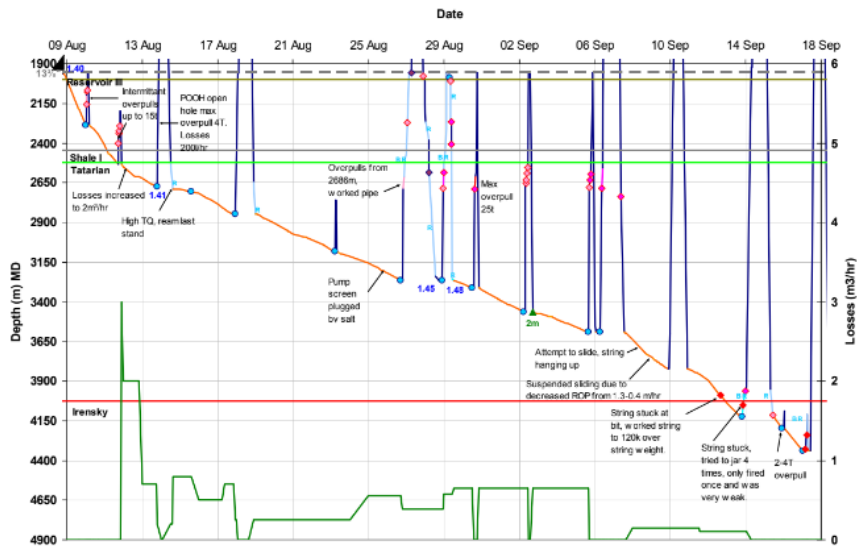


Figure 5-Well X-88- 12 1/4" Section

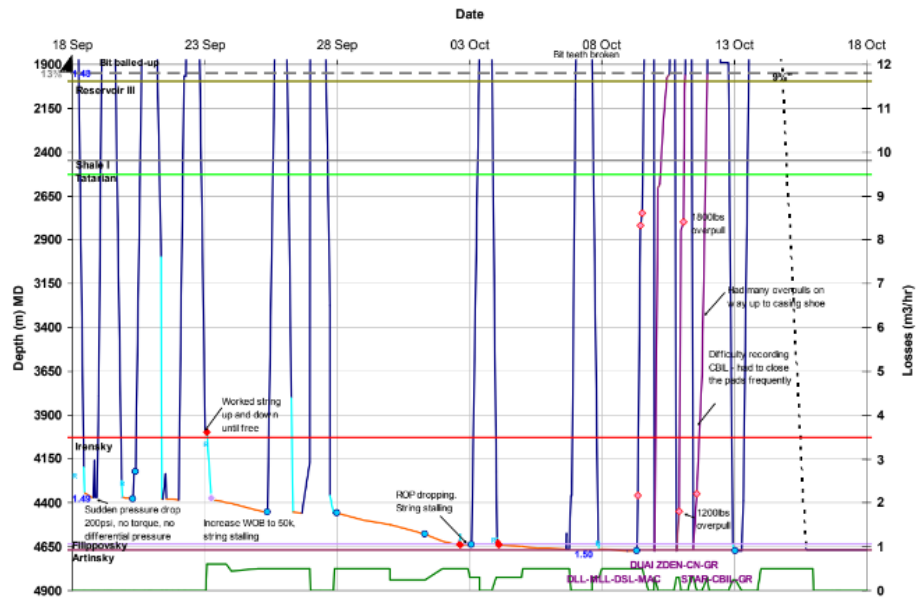


Figure 6-Well X-88- 12 1/4'' Section

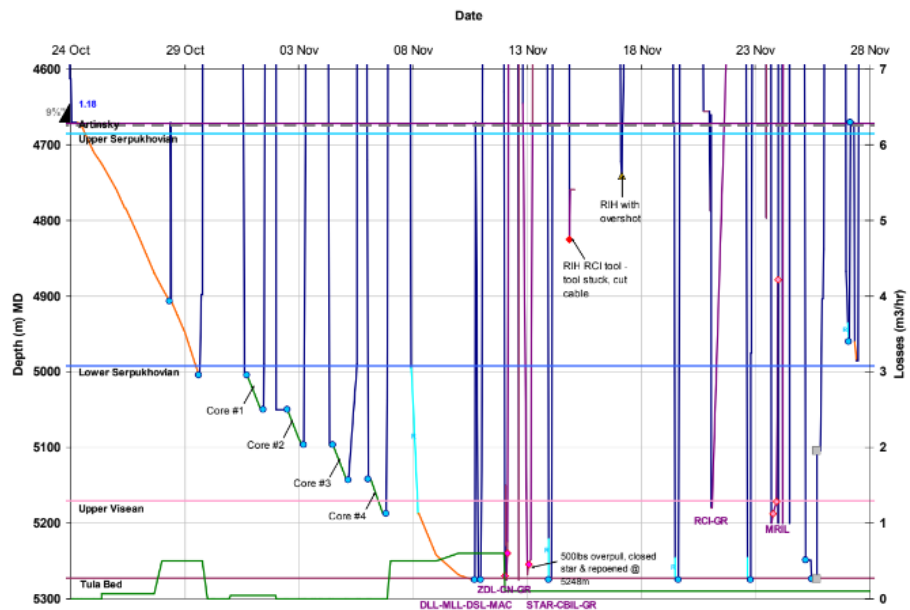


Figure 7-Well X-88- 8 1/2'' Section

3.3 Well X-77 Geomechanical Interpretation

The minor tight spots experienced in the 16'' section may indicate a limited amount of wellbore failure (breakout) in the Triassic claystones. Initially, tight spots were experienced while pulling back through the top of the Jurassic and Cretaceous. However, it is noted that no circulation was carried out prior to pulling out of hole,

therefore the tight spots encountered may have been due to inadequate hole cleaning. No tight spots were seen to recur in the section; therefore failure was likely to be limited. The losses encountered in the Triassic are likely to be seepage losses to the frequent sandstone interbeds due to the mud overbalance.

The caliper was reviewed for the 16" section and is shown in Figure 4 along with the geomechanical model predictions for each section presented as a profile. It can be seen that the well becomes progressively more overgauge towards the bottom of the section, with the caliper reading up to 20" in places. This increase in hole size corresponds to a zone where a large extent of wellbore failure is predicted in the claystone / siltstones by the geomechanical model. It is also likely that there is an 'overprint' from the reaming operations, where failed material will have been removed from the wellbore wall by mechanical disturbance and circulation.

The profile also shows the model forecasts for the 12 1/4-inch section. It can be seen that in the clays and siltstones of the III Triassic formation and in the Tatar deposit, a zone of excessive calibration is marked. The company said significant problems were noted when drilling the site, which included repeated bottlenecks, cavities, drag, and the need for expansion and reverse expansion. It is likely that extensive wellbore failure occurred in the area, although this was later stabilized when the weight of the drilling fluid was increased. CBIL log (round image of the well) was run in a 12 1/4-inch section, although logging encountered difficulties and the log was not viewable.

The hole appears to be closer to the calibration in Kazansky, then increases in diameter in Irensky, which is due to the destruction of the clay layers in the salt. The upper part of the site was opened for 46 days during logging operations. Therefore, it is likely that the degree of well failure has increased over time, as well as as a result of disturbances during multiple trips. Such effects can be carefully analyzed, but the focus of the current work has been on identifying the underlying failure processes. Very few drilling problems were experienced in the 8 1/2" section. However, a CBIL (Circumferential Borehole Imaging) was available for viewing, which indicated widespread destruction of the borehole throughout the section. An example of the extent of the breakout observed in the Upper Serpukhov is shown in Figure 9 for the zone between 4709-4714.8 m A.D. The lithology is described as dolomitic limestone in the composite log, and the caliper is also above the gauge in this section. The image log shows that the hole was intact in the Lower Serpukhovsky, although the underlying Upper vise and significantly failed. These observations are reflected in the model forecasts.

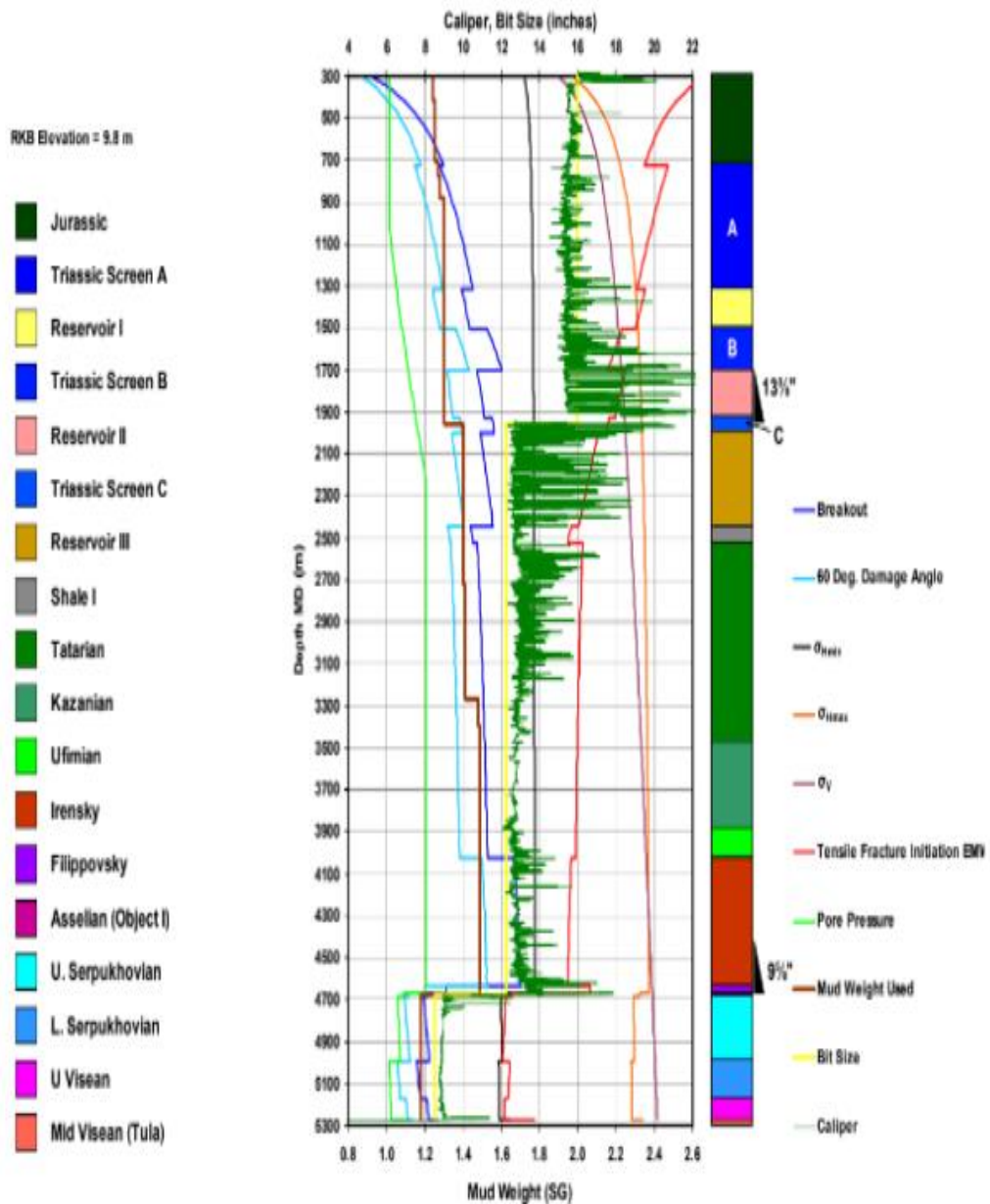


Figure 8- Model Prediction and Caliper Comparison for Well X-77

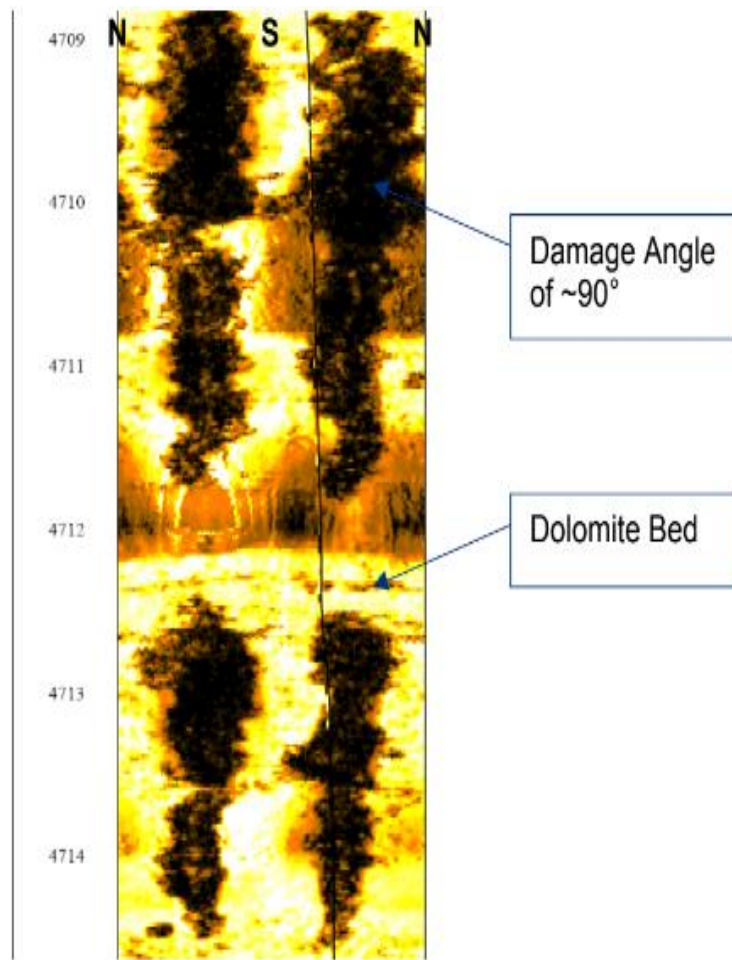


Figure 9-CBIL Log Showing Breakout in the Upper Serpukhovian of Well X-88

Database

The essential parameters for assessing the mechanical stability of a wellbore in any lithology are:

- The depth trend of the magnitudes of the in situ principal stresses.
- The depth trend of the azimuths of the in situ principal stresses.
- The depth trend of the pore pressure.

The properties describing the mechanical strength of the material.

For this assessment, the main stresses at the site were assumed to be oriented vertically and horizontally, with the values of the vertical stresses being equivalent to the overburden pressure. These premises imply that the total stress field at a point is determined with knowledge of the 3 main stress values and the azimuth of one of the horizontal stresses. It is possible that the rotation of the stress axes in situ may occur near the salt wall. The degree of rotation is hard to obtain. On the other hand, due to the steep sides of both salt walls, the rotation is likely to be minimal, and the change in the behavior of each formation due to this will be taken into account during calibrating the model.

Table 1- lithology, density of X-88 well

LITHO	DENS	Formation
	2,65	-
	2,67	-
	2,69	Cretaceous Salt-Free
	2,67	Jurassic Salt-Free
	2,67	Triassic Salt Free
	2,65	Triassic Salt Free
	2,67	Triassic Salt Free
	2,65	Triassic Salt Free
	2,65	Reservoir I Salt-Free
	2,65	Reservoir I Salt-Free
	2,67	Reservoir II Salt-Free
	2,67	Reservoir II Salt-Free
	2,65	Reservoir III Salt-Free
	2,65	Shale I Salt-Free
	2,67	Tatarian Salt-Free
	2,67	Tatarian Salt-Free
	2,65	Tatarian Salt-Free
	2,69	Tatarian Salt-Free
	2,69	Tatarian Salt-Free
	2,67	Kazanian Salt-Free
	2,65	Kazanian Salt-Free
	2,69	Ufimian
	2,65	Ufimian
	2,67	Irenskiy Salt-Free
	2,69	U.Serpukhovean SF
	2,65	U.Serpukhovean SF
	2,65	U.Serpukhovean SF
	2,69	L.Serpukhovean SF
	2,84	L.Serpukhovean SF

a. Stresses and Pore Pressure

The processed Formation Integrity Test (FIT) and Leakoff Test (LOT) results were part of the data reviewed for this study by the company representatives. The dataset for the X Field is limited. The dataset reviewed included six FITs and one LOT. The resulting LOT and FIT pressures were then plotted and a trend line fitted to the data. This trend line was then used to give an approximate σ_{Hmin} TVDbgl relation, which was used in the Salt-Free Model due to the location of the well that the tests were carried out in.

$$\text{Overburden } \sigma_{hmin} = 2.526 \cdot \text{TVDbgl} \quad , \quad (1)$$

where σ_{hmin} – minimum horizontal stress, psi;

TVDbgl – true vertical depth below ground level, m.

$$\text{Reservoir } \sigma_{hmin} = 2.348 \cdot \text{TVDbgl} \quad . \quad (2)$$

The LOT, FIT values and σ_{hmin} TVDbgl trend by engineers of X-field used in each model are shown below in Figure 10

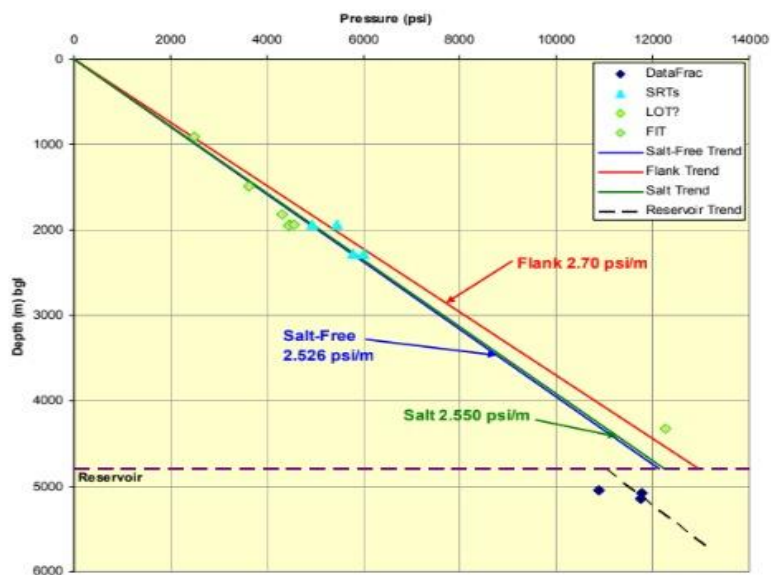


Figure 10-The LOT, FIT values and SHmin TVDbgl trend

b. Initial input data

Initially values of true vertical depth (TVD), vertical stress (σ_v), maximum and minimum horizontal stresses (σ_{Hmax} , σ_{hmin}) given and provided by X-field engineers which is shown below in Table 2.

Table 2- True vertical depth (TVD), vertical stress (σ_v), maximum and minimum horizontal stresses (σ_{Hmax} , σ_{hmin}) values.

TVD, m	Sv , psi	Sh min, psi	Sh max, psi
0	0	0	0
100	207,44	252,6	191,1
300	841,1	757,8	873,3
500	1479,56	1263	1555,5
700	2122,82	1768,2	2237,7
900	2770,88	2273,4	2919,9
1100	3423,74	2778,6	3602,1
1300	4081,4	3283,8	4284,3
1500	4743,86	3789	4966,5
1700	5411,12	4294,2	5648,7
1900	6083,18	4799,4	6330,9
2100	6760,04	5304,6	7013,1
2300	7441,7	5809,8	7695,3
2500	8128,16	6315	8377,5
2700	8819,42	6820,2	9059,7
2900	9515,48	7325,4	9741,9
3100	10216,34	7830,6	10424,1
3300	10922	8335,8	11106,3
3500	11632,46	8841	11788,5
3700	12347,72	9346,2	12470,7
3900	13067,78	9851,4	13152,9
4100	13792,64	10356,6	13835,1
4300	14522,3	10861,8	14517,3
4500	15256,76	11367	15199,5
4700	15996,02	11872,2	15881,7
4800	16367,45	12124,8	16222,8
4900	16740,08	12377,4	16563,9
5000	17113,91	12630	16905
5100	17488,94	12882,6	17246,1

Porosity calculations:

$$\varphi = (\rho_{mat} - \rho_b) \div (\rho_{mat} - \rho_{fl}), \quad (3)$$

where φ – porosity,

ρ_{mat} – matrix density, g/cm³

ρ_b – bulk density, g/cm³

ρ_{fl} – fluid density, g/cm³

$\rho_{fl}=1,094$ g/cm³.

Log density calculations:

$$\rho_{log} = (\sigma_{v2} - \sigma_{v1}) \div (8,35 \cdot 0,052 \cdot (TVD_2 - TVD_1)) \quad (4)$$

where ρ_{\log} – density of log, g/cm³

Porosity from log density:

$$\varphi_{\log \text{ dens}} = (\rho_{\text{mat}} - \rho_{\log}) \div (\rho_{\text{mat}} - \rho_{\text{fl}}); \quad (5)$$

where $\varphi_{\log \text{ dens}}$ – porosity from log density

Hydrostatic pore pressure:

$$P_{p1_hydro} = 1 \cdot 8,35 \cdot 0,052 \cdot \text{TVD} \quad (6)$$

$$P_{p2_hydro} = P_{p1_hydro} + 1 \cdot 8,35 \cdot 0,052 \cdot (\text{TVD}_2 - \text{TVD}_1) \quad (7)$$

where P_{p_hydro} – hydrostatic pore pressure, psi

Theoretical porosity:

$$\varphi_{\text{theor}} = 0,4 \cdot \exp(-0,0002 \cdot (\sigma_v)); \quad (8)$$

Actual pore pressure:

$$P_{p_act} = \sigma_v + (1/0,0002) \cdot \text{LN}(\varphi_{\log \text{ dens}} \div 0,4) \quad (9)$$

Uniaxial Compressive Strength:

Table 3- Empirical relationships between UCS and other physical properties in sandstones. [Error! Reference source not found.] (D., 2006)

Equation No.	UCS, MPa	Region where developed	General comments	Reference
1	$0.035 V_p - 31.5$	Thuringia, Germany	–	(Freyburg 1972)
2	$1200 \exp(-0.036 \Delta t)$	Bowen Basin, Australia	Fine grained, both consolidated and unconsolidated sandstones with wide porosity range	(McNally 1987)
3	$1.4138 \times 10^7 \Delta t^{-3}$	Gulf Coast	Weak and unconsolidated sandstones	Unpublished
4	$3.3 \times 10^{-20} \rho^2 V_p^2 [(1+\nu)/(1-\nu)]^2 (1-2\nu) [1+0.78V_{\text{clay}}]$	Gulf Coast	Applicable to sandstones with UCS > 30 MPa	(Fjaer, Holt <i>et al.</i> 1992)
5	$1.745 \times 10^{-9} \rho V_p^2 - 21$	Cook Inlet, Alaska	Coarse grained sands and conglomerates	(Moos, Zoback <i>et al.</i> 1999)
6	$42.1 \exp(1.9 \times 10^{-11} \rho V_p^2)$	Australia	Consolidated sandstones with $0.05 < \phi < 0.12$ and UCS > 80MPa	Unpublished
7	$3.87 \exp(1.14 \times 10^{-10} \rho V_p^2)$	Gulf of Mexico	–	Unpublished
8	$46.2 \exp(0.000027E)$	–	–	Unpublished
9	$A(1-B\phi)^2$	Sedimentary basins worldwide	Very clean, well consolidated sandstones with $\phi < 0.30$	(Vernik, Bruno <i>et al.</i> 1993)
10	$277 \exp(-10\phi)$	–	Sandstones with $2 < \text{UCS} < 360$ MPa and $0.002 < \phi < 0.33$	Unpublished

Units used: V_p (m/s), Δt ($\mu\text{s}/\text{ft}$), ρ (kg/m^3), V_{clay} (fraction), E (MPa), ϕ (fraction)

Table 4-Empirical relationships between UCS and other physical properties in sandstones. [Error! Reference source not found.] (D., 2006)

	UCS, MPa	Region where developed	General comments	Reference
11	$0.77 (304.8/\Delta t)^{2.93}$	North Sea	Mostly high porosity Tertiary shales	(Horsrud 2001)
12	$0.43 (304.8/\Delta t)^{3.2}$	Gulf of Mexico	Pliocene and younger	Unpublished
13	$1.35 (304.8/\Delta t)^{2.6}$	Globally	–	Unpublished
14	$0.5 (304.8/\Delta t)^3$	Gulf of Mexico	–	Unpublished
15	$10 (304.8/\Delta t - 1)$	North Sea	Mostly high porosity Tertiary shales	(Lal 1999)
16	$0.0528E^{0.712}$	–	Strong and compacted shales	Unpublished
17	$1.001\phi^{-1.143}$	–	Low porosity ($\phi < 0.1$), high strength shales	(Lashkaripour and Dusseault 1993)
18	$2.922\phi^{-0.96}$	North Sea	Mostly high porosity Tertiary shales	(Horsrud 2001)
19	$0.286\phi^{-1.762}$	–	High porosity ($\phi > 0.27$) shales	Unpublished

Units used: Δt ($\mu\text{s}/\text{ft}$), E (MPa), ϕ (fraction)

Poisson's ratio:

$$\text{Poisson's ratio} = ((\sigma_{\text{hmin}} - P_{\text{p_act}}) \div (\sigma_{\text{v}} - P_{\text{p_act}})) \div (1 + (\sigma_{\text{hmin}} - P_{\text{p_act}}) \div (\sigma_{\text{v}} - P_{\text{p_act}})) \quad (10)$$

Young's modulus, GPa:

Table 5-Young's Modulus for different formations. [Error! Reference source not found.] (Ocak, 2009)

Formation	Number of data	Equations*	r
Mudstone	47	$E_1 = 0.3436\text{UCS}^{0.8721}$ (Eq. 1)	0.884
Diabase	13	$E_1 = 0.1627\text{UCS}^{1.0588}$ (Eq. 2)	0.942
Claystone	40	$E_1 = 0.3485\text{UCS}^{0.8866}$ (Eq. 3)	0.837
Limestone	76	$E_1 = 0.4153\text{UCS}^{0.8692}$ (Eq. 4)	0.935
Conglomerate	13	$E_1 = 1.1329\text{UCS}^{0.5761}$ (Eq. 5)	0.849
Sandstone	180	$E_1 = 0.3341\text{UCS}^{0.8818}$ (Eq. 6)	0.893
Siltstone	12	$E_1 = 6.7152e^{0.0131\text{UCS}}$ (Eq. 7)	0.639

* E_1 : GPa, UCS : MPa

Table 6-Statistical relationships for estimation of modulus of elasticity for different geologic formations and all formations together [[Error! Reference source not found.](#)] (Ocak, 2009)

Equations	Number of data	Formation	Lithology	r
$E_i = 0.3663UCS^{0.8213}$ (1)	73	Trakya	Sandst.-siltst.-clayst.	0.915
$E_i = 1.0331UCS^{0.8443}$ (2)	8	Tuzla	Shale	0.903
$E_i = 0.7498UCS^{0.6495}$ (3)	38	Kartal	Shale-limestone	0.747
$E_i = -24.7 + 0.102UCS + 1.1\gamma$ (4)	20	Kurtköy	Sandstone-conglomerat.	0.908
$E_i = 2.0562UCS^{0.5238}$ (5)	34	Dolayoba	limestone	0.478
$E_i = 0.5342UCS^{0.7672}$ (6)	177	All form.	All lithology above	0.809
$E_i = \frac{CP^{2.885}}{10^4}$ $CP = \frac{\ln UCS^{0.689} \ln \gamma^{4.95}}{16.6}$ (7)	177	All form.	All lithology above	0.834

RESULTS

6.1.1 Offset Well Behaviour

When a well is drilled in a stressed environment, the stress around the well increases due to the removal of stress-bearing material existing at that location. Breakouts in a well are formed when the stresses near the well exceed the rock strength. A breakout within the sandstone blocks occurs only occasionally, and therefore, where intertwined sands and clays meet, a borehole profile is formed. This leads to problems with disconnecting, cleaning holes, and starting the casing.

Limited amounts of breakout in reservoir formations were observed on image logs. However, image log quality was variable due to observations many logs being pipe-conveyed. Notwithstanding this, drilling problems within reservoir formations are rare, showing that breakout is not 'progressive' and stabilises providing that drilling disturbance in failed zones is limited.

6.1.2 Sensitivity analysis

A sensitivity analysis determines how different values of an independent variable affect a particular dependent variable under a given set of assumptions. In other words, sensitivity analyses study how various sources of uncertainty in a mathematical model contribute to the model's overall uncertainty. This technique is used within specific boundaries that depend on one or more input variables. **[Error! Reference source not found.]** (Kenton, 2019)

Sensitivity analysis is a method for evaluating the stability of a system. It links the uncertainty at the model's output to various sources of uncertainty at the model's input. The sensitivity of each factor was studied by changing its value in a given range while keeping all other factors constant at their base value. Sensitivity analysis describes the system sensitivity to a single factor. A real-world system character (such as wellbore stability in this study) is governed by several factors (in-situ stresses, geomechanical properties) with various physical quantities and units.

To calculate the displacement (U_{max}) of the well, the Equations 13-18 were used. The equations selected from a set of possible selected curves in order to estimate the displacement of the wellbore walls as close as possible to the numerical results. These adjusted equations are used to quantify the sensitivity of each factor. The sensitivity of the displacement of the well walls is a criterion of resistance to the factors of these types of rocks. The displacement of the well walls is practically not sensitive to changes in vertical stresses, so they are not shown in Fig.11. As expected, the displacement of the borehole walls increases (i.e. the stability of the well

decreases) due to an increase in internal stress and pore pressure, while an increase in the pressure of the drilling fluid or the pressure in the well reduces the displacement of the well walls (i.e., increases the stability of the well). As shown in Figure 8, an increase in the minimum horizontal stress led to a decrease in displacement, i.e., an increase in stability. An increase in the minimum horizontal stress resulted in a decrease in the displacement for the strong rock type in Figure 9. When the minimum horizontal stress increases, a more uniform stress field occurs, i.e. lithostatic stress field. This increases the stability of the well for weak rocks. Since the maximum horizontal stress in this analysis is constant, a greater increase in the minimum horizontal stress results in a higher stress concentration around the wellbore. This eventually led to higher displacements in the well wall, as it is increasingly controlled by plastic properties rather than elastic ones. The maximum horizontal stress appears to have a significant effect on the stability of the wellbore, as results change rapidly.

$$U_{max} = (26.7 + 0.445 * S_{hmin}) * 10^{-3} + \frac{9.63}{S_{hmin}} \quad (11)$$

$$U_{max} = 10.4 * 10^{-3} * S_{Hmax} - 0.4298 \quad (12)$$

$$U_{max} = (1.27 * P_p^3 - 97.1 * P_p^2 + 2217 * P_p + 22400) * 10^{-6} \quad (13)$$

$$U_{max} = (534 - 8 * P_w) * 10^{-3} \quad (14)$$

$$U_{max} = \frac{3.642}{E} \quad (15)$$

$$U_{max} = 0.11 * \nu + 0.22 \quad (16)$$

S_{hmin} – Minimum horizontal stress

S_{Hmax} – Maximum horizontal stress

P_p – Pore pressure

U_{max} – Maximum wellbore displacement

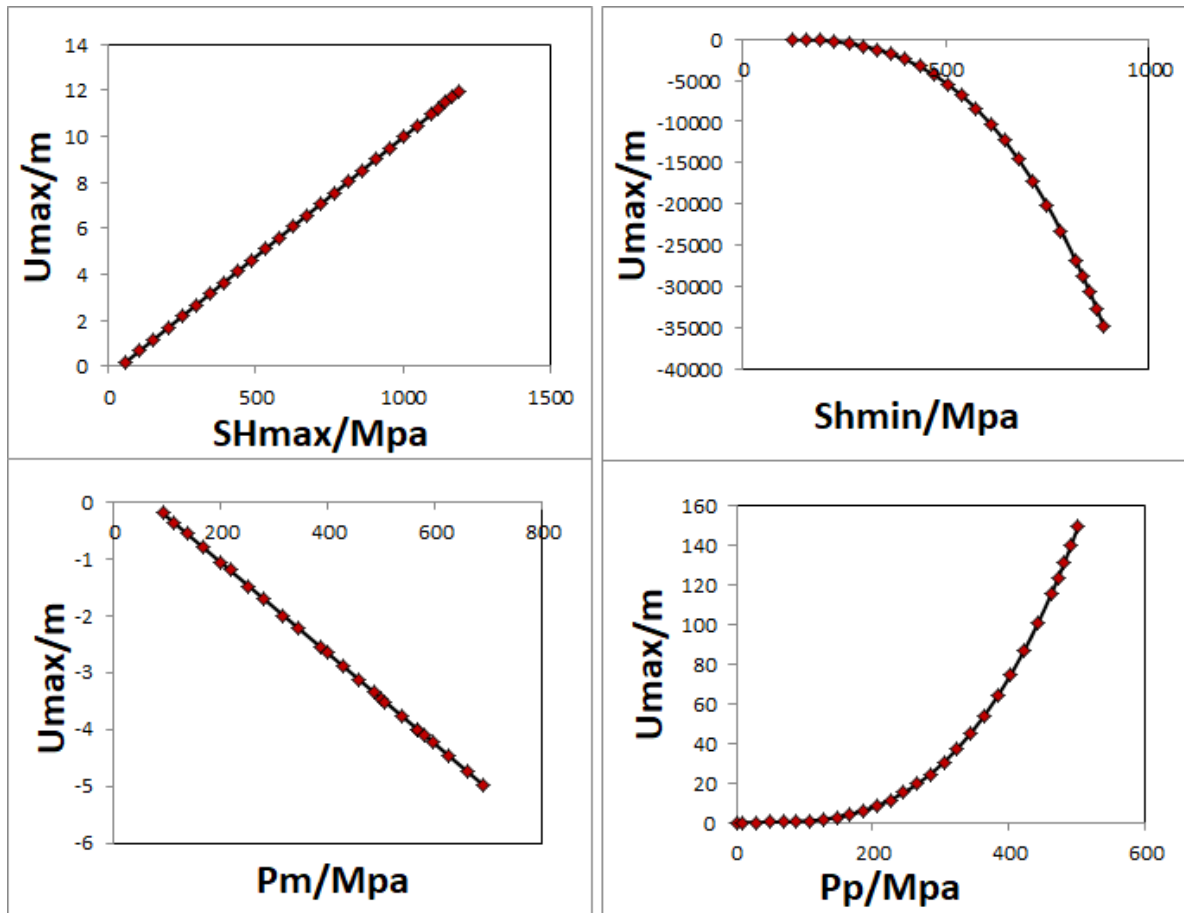


Figure 11- Sensitivity analysis of in-situ stresses and pressures

Figure 12 shows the effect of geomechanical properties on wellbore stability. The increase in geomechanical properties reduced the stability of the wellbore in all cases, except for the case of the Poisson's ratio. Increasing the Poisson's ratio increased the displacement of the wellbore. Poisson's ratio is usually determined using well-logging, fracturing data and core samples. In our case we found out using Eq(12). As all we know, Poisson's Ratio, ν is the fraction of expansion divided by the fraction of compression. When a material is compressed in one direction, it usually tends to expand in the other two directions perpendicular to the direction of compression. Accordingly, as Poisson's ratio increases, as the displacement of the wellbore increases.

Also in Figure 12 we can see how displacement changes within Young's modulus. Elastic modulus is a number that depicts an object or substance's resistance from being deformed elastically (i.e., non-for all time) toward the force, when a force is applied to it. It is additionally known by various different names, for example, modulus of flexibility or Young's modulus. So, it increases the stress on an object, and decides how it strains (i.e twists) and by increasing Young's modulus, the displacement of the wellbore decreases. .

The exact solution for the most sensitive parameters cannot be given only on the basis of Figure 11 and Figure 12, since the factors under study have different units of measurement and range of variation. Sensitivity analysis requires establishing a relationship between the studied factor (for example, the modulus of elasticity) and the nature of the system (for example, the stability of the wellbore).

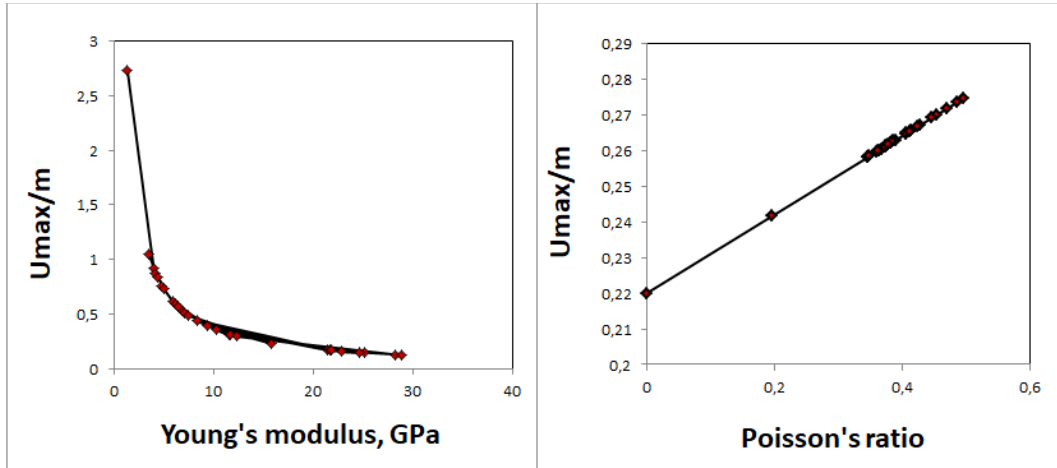


Figure 12-Sensitivity analysis of geomechanical factors

For more accurate results, we performed another sensitivity analysis. Sensitivity analysis was conducted with the @RISK Excel, a program that provides calculation of the risk severity using Monte Carlo simulations to show probabilities of specific input parameters. For each input parameter, probable ranges are determined by considering variations of input data as described in Table 7.

Table 7-Input data ranges for the wellbore-stability sensitivity analysis

	Actual	Min	Most likely	Max
Sh max, Mpa	607,1129	13,186	618,17195	1189,9809
Pp_hydr, Mpa	257,7562	9,8268	262,27429	501,16753
Sh min, Mpa	457,1712	17,429	465,18468	888,8994
Mud pressure, Mpa	350,7246	12,375	352,00595	687,79303
Poisson's ratio	0,356772	0,1957	0,3780594	0,496528
Young's modulus, GPa	13,98268	1,3348	11,758382	28,854884

The breakout pressure (P_b) is a criterion of stability in wellbore-stability sensitivity analysis. To find breakout pressure Equations 19-23 were used.

$$P_b = 3S_{hmin} - S_{Hmax} - P_p \quad (17)$$

$$S_{hmin} = \frac{(S_{Hmax} + 2P_p + dP + \sigma dT)}{3} ; dP = P_m - P_p \quad (18)$$

$$S_{Hmax} = \frac{(C_o + 2P_p + dP + \sigma dT) - S_{hmin}(1 + 2\cos 2\theta b)}{(1 - 2\cos 2\theta b)} ; 2\theta b = \pi - w_{bo} ; w_{bo} = 600 \quad (19)$$

The probability of happening breakout in 10% and 90% values are simulated using @RISK Excel identify key driving factors at given uncertainties to prevent breakouts. The results of the probability density simulation are shown in Fig. 13. To prevent a breakthrough, a 10% value of 345 MPa was calculated, and a 90% value of 1298 MPa.

It is necessary to evaluate the sensitivity of the output data to see the dominant parameters that affect the wellhead breakouts. In Figure 13, the tornado diagram shows that the most dominant parameters that affect the prevention of hole rupture are horizontal stresses, pore pressure, and UCS. Based on this sensitive analysis, the present study has focused on collecting baseline data, and future research should continue to focus on reliable geomechanical data and on-site underlying stresses.

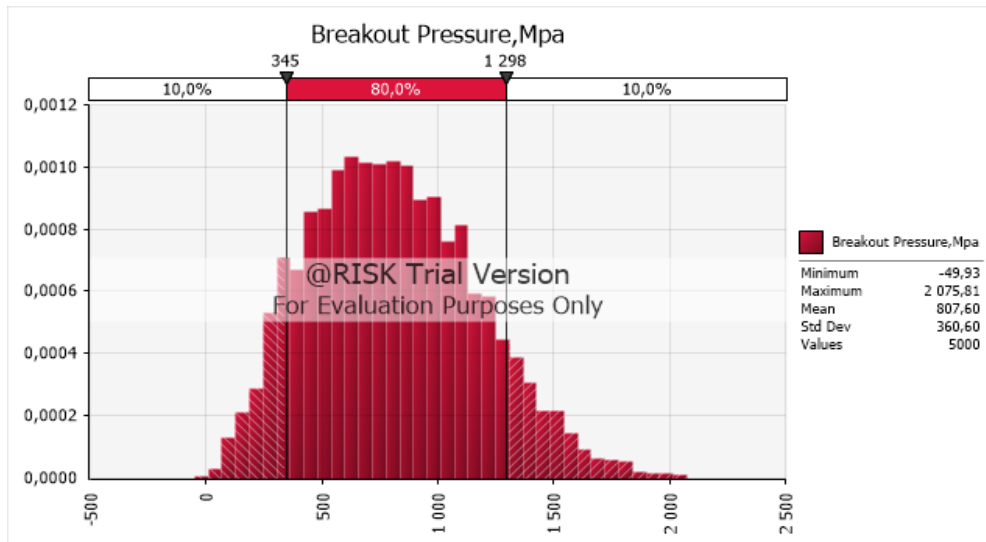


Figure 13-Probability of breakout pressure.

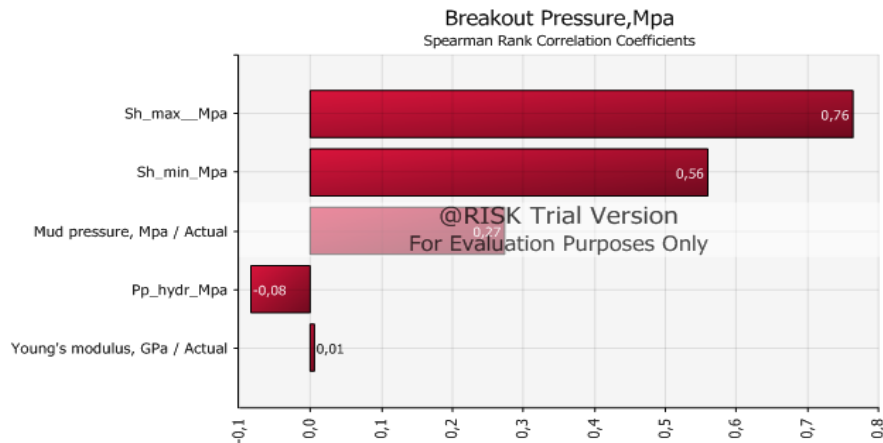


Figure 1- Contribution of various input parameters to minimum pressure to prevent breakouts

A dimensionless sensitivity analysis on the stability of the borehole was performed. The extreme displacement of the borehole partition is chosen as the principle of immutability (i.e., wells with a higher displacement are considered unstable). dimensionless sensitivity analysis, using the hypersensitivity factor, allowed us to quantify the share of misconceptions in the way of thinking about the immutability of the wellbore, based on the discrepancy between the input geomechanical components and the stresses and pressures in place. As a result, it was found that accentuation at the highest level is practically an effective factor. due to the perpendicular borehole being a euphemistic former when looking at the most extreme level of accentuation, hawthorn will be common to the most extreme representation of accentuation, common to the axis of the borehole. Poisson matching always has a bit of an over-sensitivity to the results.

Risk analysis shows that the key parameters in determining the correct average weight to prevent well breakouts and tensile fractures are:

- The in situ principle stresses magnitudes and orientations;
- Uniaxial compressive strength;
- Pore pressure;
- Internal friction angle of the formation;

CONCLUSIONS AND RECOMMENDATION

7.1 Conclusion

- This work allows you to predict and prevent, reduce periods of wellbore instability in progression to reduce production costs and life-threatening conditions. The resulting collection region estimates and day-to-day production descriptions should be euphemistic in order to influence the variability of weather conditions in the wellbore. Geomechanical psychoanalysis has far-reaching implications for reducing the duration of no-load production (NPT). The interpretation of the borehole condition for each position was based on the daily drilling reports, caliper logs and the interpretation of image logs. Test points within the geomechanical model have been graded for quality depending upon the amount of information that was available for each test point. The higher confidence test points are normally given to those where a problem is repeatedly seen, where caliper confirms reported problems or orientated four / six arm caliper or image logs are available.
- A dimensionless sensitivity analysis is performed on wellbore stability. The maximum wellbore wall displacement is chosen as the stability criterion (i.e., wellbores with higher displacement considered more unstable). The results of this study may be used in oilfields planning. Taking into account the overall strength of the formations, engineers can plan on the number of needed geomechanical samples and tests for deriving the properties of the field, saving costs on low sensitive parameters and investing on most effective parameters.
- Continuous updating of geomechanical models leads to more accurate predictions, therefore better models.
- According to advise of field engineers some drilling guidelines supposed to mitigate:

Hole cleaning: The emphasis while drilling sensitive formations should be to maintain a clean annulus to prevent packing off tight spots and stuck pipe. The key element in recognizing whether the hole is being cleaned properly is observation of the returns at the shale shakers. Any deviation from the normal trend must be reported to the drill floor immediately. This may indicate poor hole cleaning (reduction in cuttings) or hole instability (increase in cuttings, cavings).

Circulation rates must be sufficient at all times to clean the hole but not to cause erosion of the sands particularly in the Jurassic. The actual flow rate will be established by experience, but it is recommended that the following minimum flow rates be used where it is known that breakout may be occurring.

ECD (Equivalent Circulating Density) Monitoring is the key to successfully drilling weak formations. It is best achieved by use of a PWD tool in the BHA (Bottom Hole Assembly) because any swab and surge incidents can be instantly seen and repetition avoided. It is also the easiest way to know whether or not the annulus is being loaded with cuttings or cavings.

Glossary

Allowable damage angle: The damage angle that a wellbore can tolerate while still able to be successfully cleaned.

Breakout: Compressive failure experienced in the wellbore wall. In anisotropic stress conditions this leads to wellbore enlargement in the minimum horizontal stress direction. In isotropic stress conditions breakout leads to a uniform wellbore enlargement. The failed rock forms carvings.

Breakout mud weight: The minimum mud weight that is accurate to prevent wellbore breakout.

Cavings: Rock that originates from the borehole wall cause of borehole instability.

Compressive stress: Stress that squeezes and crushes sooner than pulls apart.

Damage angle: Half of the sum of all angles subtended at the mid of the circular wellbore by circumferential arcs of breakout.

Deviated well: Well with a trajectory with inclinations more than 10°.

Fracture initiation pressure: The pressure at which new fractures are formed in undisturbed rock formations by tensile failure.

In situ stress: Stress that is present naturally within a rock mass.

Linear elasticity: Deformation that follows a linear relationship with applied stress. Once the stress is removed rock properties return to their original state providing the elastic limit has not been exceeded.

Minimum safe mud weight: The minimum mud weight required to prevent wellbore breakout (see breakout mud weight).

Offset well: An existing well considered to have penetrated sufficiently similar formations to those anticipated for the proposed well to be used in the design of the proposed well.

Overburden stress (σ_V): The vertical component of stress at a point due to the weight of overlying formations.

Poisson's ratio: The ratio of lateral elastic strain to longitudinal elastic strain experienced by an object undergoing elastic deformation.

Pore pressure: The pressure of the fluid filling the formation porosity. This is known as formation pressure in non-reservoir formations and reservoir pressure within reservoir rocks.

Principal stresses: Three orthogonal stress components that define the stress tensor at a given location, comprising the maximum stress magnitude, the minimum stress magnitude, and the intermediate stress magnitude. The 3 shear stress magnitudes reduce to zero in the principal stress directions.

Strain: The ratio of change in length to original length caused by applied stress.

Strength: The property of a material that maintains the material in mechanical equilibrium when subjected to stress.

Stress: A force (load) applied to an object expressed as magnitude per unit area. At a given location within the object the stress magnitude varies with orientation. Stress is described by 6 stress components, being 3 shear stress components and 3 normal stress components, all with potentially different magnitudes. Where the object is a body of non viscous fluid the shear stress components are zero and the normal stress components are all equal, in this special case stress is known as pressure.

Stress path parameter, K: The ratio of change in effective horizontal stress to change in effective vertical stress.

Tensile: Stress that pulls apart and separates.

Tensile mud weight: The mud weight at which new fractures are initiated.

Tensile failure: The breakdown of the fabric of the material leading to fractures caused by stress components pulling the material apart and exceeding the tensile strength of the material.

Tornado diagram: A common tool used to depict the sensitivity of a result to changes in selected variables. It shows the effect on the output of varying each input variable at a time, keeping all the other input variables at their initial (nominal) values.

Uniaxial: Having one axis. With reference to rock mechanics, 'uniaxial' refers to the application of stress in one axis only, normally the long axis of a core specimen with no stress applied in the other axes, i.e. around the core specimen.

Uniaxial compressive strength (S_c): Strength value derived from uniaxial compressive testing of prepared core samples. Correlation exists between wireline logging measurements and S_c . Strength is typically measured in psi

ABBREVIATIONS

B	Breakout test point
CALI	Single arm caliper data
DA	Wellbore damage angle
ΔP	Change in Formation Pressure
Δt	Delta t (sonic interval transit time)
ECD	Equivalent circulating density
EMW	Equivalent mud weight
FIT	Formation integrity test
ft	Feet
GR	Gamma ray
LCM	Loss circulation material
LO	Losses test point
LOT	Leak off test
MD	Measured depth
MPa	Mega (x10 ⁶) Pascals
ν	Poisson's ratio
NB	No breakout test point
NOLO	No losses test point
NOT	No tensile failure test point
Nphi	Porosity data
OBM	Oil based mud
OK	No geomechanical stability issues, test point
POSNB	Possibly no breakout test point
PP	Formation pore pressure test point
Pp	Formation pressure
ppg	Pounds per gallon
psi	Pounds per square inch
Rhob	Bulk density
SC	Uniaxial compressive strength
SG	Specific Gravity
σ_{Hmax}	Maximum horizontal stress
σ_{Hmin}	Minimum horizontal stress
σ_V	Vertical stress
T	Tensile failure (breakdown) test point
TD	Total Depth, either hole section TD or total depth of the well.
TVDRKB	True vertical depth relative to RKB
TVDss	True vertical depth relative to mean sea level (sub sea)
UCS	Uniaxial Compressive Strength
WBM	Water based mud

REFERENCES

- Ahangari, K. (2017). *ResearchGate*. Retrieved from Effects of different stress regimes on hydraulic fracture geometry: a particle flow code approach: https://www.researchgate.net/figure/Different-faulting-stress-regimes-a-Normal-fault-regime-b-Strike-slip-fault-regime_fig2_318220870
- Bigoni, F. (2010). *OnePetro*. Retrieved from Karachaganak Field - Dynamic Data to drive geological modelling: <https://www.onepetro.org/conference-paper/SPE-139881-MS>
- D., Z. M. (2006). *Empirical relations between rock strength and physical*. Retrieved from Journal of Petroleum Science and Engineering 51: https://pangea.stanford.edu/departments/geophysics/dropbox/STRESS/publications/MDZ%20PDF's/2006/2006_Empirical_relations_between_rock_strength.pdf
- Kenton, W. (2019). *Investopedia* . Retrieved from Sensitivity analyses: <https://www.investopedia.com/terms/s/sensitivityanalysis.asp>
- Mohammad, F. (2018, August). *International Journal of Engineering and Technology (IJET)* . Retrieved from Investigating the Stability of the Wellbore: <http://www.enggjournals.com/ijet/docs/IJET18-10-04-218.pdf>
- Ocak. (2009). *ResearchGate*. Retrieved from Empirical Estimation of Intact Rock Elastic Modulus: https://www.researchgate.net/publication/259975436_Empirical_Estimation_of_Intact_Rock_Elastic_Modulus
- PetroWiki. (2015). *Subsurface stress and pore pressure*. Retrieved from PetroWiki: https://petrowiki.org/Subsurface_stress_and_pore_pressure
- Zoback, M.D., Barton, C.A., Castillo, D.A., Finkbeiner, T., Grollmund, B.R., Moos, D.B., Wiprut, D.J., Brudy, M., Ward, C.D., & Pesca, P. (2003). "Determination of stress orientation and magnitude in deep wells"

Appendix A

OFFSET DATA USED IN DIPLOMA PROJECT

Table A

TVD, m	TVD, FT	LITHO	DENS	Formation	LOG DENS, G/CC	LOG DENS, G/CC
0	0		2,65	-	0	0
100	328		2,67	-	1,34517195	1,45656155
300	984		2,69	Cretaceous Salt-Free	2,401036903	2,22465482
500	1640		2,67	Jurassic Salt-Free	2,401036903	2,24150667
700	2296		2,67	Triassic Salt Free	2,401036903	2,25835852
900	2952		2,65	Triassic Salt Free	2,401036903	2,27521037
1100	3608		2,67	Triassic Salt Free	2,401036903	2,29206222
1300	4264		2,65	Triassic Salt Free	2,401036903	2,30891407
1500	4920		2,65	Reservoir I Salt-Free	2,401036903	2,32576592
1700	5576		2,65	Reservoir I Salt-Free	2,401036903	2,34261777
1900	6232		2,67	Reservoir II Salt-Free	2,401036903	2,35946962
2100	6888		2,67	Reservoir II Salt-Free	2,401036903	2,37632147
2300	7544		2,65	Reservoir III Salt-Free	2,401036903	2,39317332
2500	8200		2,65	Shale I Salt-Free	2,401036903	2,41002517
2700	8856		2,67	Tatarian Salt-Free	2,401036903	2,42687702
2900	9512		2,67	Tatarian Salt-Free	2,401036903	2,44372886
3100	10168		2,65	Tatarian Salt-Free	2,401036903	2,46058071
3300	10824		2,69	Tatarian Salt-Free	2,401036903	2,47743256
3500	11480		2,69	Tatarian Salt-Free	2,401036903	2,49428441
3700	12136		2,67	Kazanian Salt-Free	2,401036903	2,51113626
3900	12792		2,65	Kazanian Salt-Free	2,401036903	2,52798811
4100	13448		2,69	Ufimian	2,401036903	2,54483996
4300	14104		2,65	Ufimian	2,401036903	2,56169181
4500	14760		2,67	Irenskiy Salt-Free	2,401036903	2,57854366
4700	15416		2,69	U.Serpukhovean SF	2,401036903	2,59539551
4800	15744		2,65	U.Serpukhovean SF	2,401036903	2,6080344
4900	16072		2,65	U.Serpukhovean SF	2,401036903	2,61646033
5000	16400		2,69	L.Serpukhovean SF	2,401036903	2,62488625
5100	16728		2,84	L.Serpukhovean SF	2,401036903	2,63331217

Table A continued

Sh max, psi	Sh max, Mpa	Umax,m Shmax	mud weight, SG	mud weight, ppg	mud pressure, Psi	mud pressure, Mpa	Umax,m mud pressure
0	0	-0,4298	0	0	0	0	0,534
191,1	13,1859	-0,292667	1,26	10,515209	179,3474	12,37497	0,435000
873,3	60,2577	0,19688	1,26	10,515209	538,0422	37,12491	0,237000
1555,5	107,3295	0,686427	1,27	10,598663	903,8539	62,36592	0,035072
2237,7	154,4013	1,175974	1,33	11,099387	1325,178	91,43728	-0,197498
2919,9	201,4731	1,66552	1,27	10,598663	1626,937	112,2586	-0,364069
3602,1	248,5449	2,155067	1,27	10,598663	1988,478	137,2050	-0,56364
4284,3	295,6167	2,644614	1,31	10,932479	2424,036	167,2585	-0,804068
4966,5	342,6885	3,13416	1,35	11,266295	2882,369	198,8834	-1,057068
5648,7	389,7603	3,623707	1,3	10,849025	3145,696	217,0530	-1,202424
6330,9	436,8321	4,113254	1,35	11,266295	3651,000	251,9190	-1,481352
7013,1	483,9039	4,602801	1,35	11,266295	4035,316	278,4368	-1,693495
7695,3	530,9757	5,092347	1,4	11,683566	4583,322	316,2492	-1,995994
8377,5	578,0475	5,581894	1,4	11,683566	4981,872	343,7491	-2,215994
9059,7	625,1193	6,071441	1,46	12,18429	5611,011	387,1598	-2,563278
9741,9	672,1911	6,560987	1,4	11,683566	5778,972	398,7490	-2,655993
10424	719,2629	7,050534	1,41	11,76702	6221,646	429,2936	-2,900349
11106	766,3347	7,540081	1,41	11,76702	6623,043	456,99	-3,12192
1178	813,4065	8,029628	1,41	11,76702	7024,44	484,6863	-3,343491
12470	860,4783	8,519174	1,48	12,351198	7794,495	537,8201	-3,768561
13152	907,5501	9,008721	1,48	12,351198	8215,819	566,8915	-4,001132
13835	954,6219	9,498268	1,48	12,351198	8637,143	595,9628	-4,233703
14517	1001,693	9,987814	1,48	12,351198	9058,467	625,0342	-4,466274
15199	1048,765	10,47736	1,49	12,434652	9543,844	658,5252	-4,734202
15881	1095,837	10,96691	1,49	12,434652	9968,014	687,7930	-4,968344
16222	1119,373	11,21168	1,06	8,8461282	7242,219	499,7131	-3,463705
16563	1142,909	11,45645	1,18	9,8475767	8230,053	567,8736	-4,008989
16905	1166,445	11,70123	1,18	9,8475767	8398,013	579,4629	-4,101703
17246	1189,980	11,946	1,01	8,428858	7331,892	505,9006	-3,513205

Table A continued

<u>Pp_hydr</u>	<u>Pp_hydr,Mpa</u>	<u>Umax,m_Pp</u>	<u>Porosity</u>	<u>Porosity from log dens</u>	<u>Por theor</u>
0	0	0,224	0	0	0
142,4176	9,826814	0,23771	0,1156	0,76994826	0,39483189
427,2528	29,48044	0,24007	0,104377	0,29156966	0,36822535
712,088	49,13407	0,261021	0,1156	0,27188663	0,34308223
996,9232	68,7877	0,362966	0,1156	0,26119383	0,3193492
1281,7584	88,44133	0,608305	0,126824	0,24086737	0,2969727
1566,5936	108,095	1,059441	0,1156	0,23980824	0,27589911
1851,4288	127,7486	1,778777	0,126824	0,2192069	0,25607498
2136,264	147,4022	2,828715	0,126824	0,20837666	0,23744722
2421,0992	167,0558	4,271657	0,126824	0,19754642	0,21996323
2705,9344	186,7095	6,170005	0,1156	0,19703705	0,20357112
2990,7696	206,3631	8,586162	0,1156	0,18634425	0,18821981
3275,6048	226,0167	11,58253	0,126824	0,16505571	0,17385915
3560,44	245,6704	15,22151	0,126824	0,15422547	0,16044008
3845,2752	265,324	19,5655	0,1156	0,15426585	0,14791467
4130,1104	284,9776	24,67692	0,1156	0,14357306	0,13623627
4414,9456	304,6312	30,61815	0,126824	0,12173476	0,12535951
4699,7808	324,2849	37,4516	0,104377	0,13318762	0,11524044
4984,616	343,9385	45,23968	0,104377	0,12262881	0,10583653
5269,4512	363,5921	54,04478	0,1156	0,10080186	0,09710674
5554,2864	383,2458	63,92932	0,126824	0,07841381	0,08901152
5839,1216	402,8994	74,95568	0,104377	0,0909524	0,08151287
6123,9568	422,553	87,18628	0,126824	0,05675333	0,0745743
6408,792	442,2066	100,6835	0,1156	0,05803067	0,06816089
6693,6272	461,8603	115,5098	0,104377	0,05927599	0,06223926
6836,0448	471,6871	123,4408	0,126824	0,02697018	0,05945285
6978,4624	481,5139	131,7275	0,126824	0,02155506	0,05677755
7120,88	491,3407	140,3776	0,104377	0,04079809	0,05420963
7263,2976	501,1675	149,399	0,020202	0,11837791	0,05174543

Table A continued

Pp. actual	Pp. actual Mpa	Umax.m Pp	UCS	Sh min. psi	Sh min.Mpa	Umax,m Shmin
0	0	0,224	0	0	0	0
3481,7338	240,23963	14,148144	1,4705767	252,6	17,4294	4,7167
-739,82794	-51,04813	-0,324455	7,6244949	757,8	52,2882	3,7901
-450,83680	-31,10774	0,0198306	8,1601458	1263	87,147	3,9161
-8,1887805	-0,565026	0,2227161	8,7414807	1768,2	122,0058	-10,154
234,78958	16,200481	0,2402571	14,2149	2273,4	156,8646	-53,67
865,61524	59,727452	0,3019299	10,05912	2778,6	191,7234	-141,88
1074,1573	74,116859	0,4127079	21,39736	3283,8	226,5822	-290,03
1483,2738	102,34589	0,9025049	25,77862	3789	261,441	-513,38
1883,6653	129,97291	1,8798523	30,70376	4294,2	296,2998	-827,16
2542,8160	175,45431	5,0235105	14,52117	4799,4	331,1586	-1246,6
2940,6960	202,90803	8,1211429	15,67078	5304,6	366,0174	-1787,1
3015,7925	208,08968	8,8252405	48,68768	5809,8	400,8762	-2463,7
3362,9154	232,04117	12,626798	55,67976	6315	435,735	-3291,7
4055,4844	279,82843	23,260055	18,30077	6820,2	470,5938	-4286,4

Table A continued

<u>Pp. actual</u>	<u>Pp. actual. Mpa</u>	<u>Umax.m Pp</u>	UCS	<u>Sh min, psi</u>	<u>Sh min.Mpa</u>	<u>Umax.m Shmin</u>
4392,37727	303,07403	30,11568	19,80429	7325,4	505,4526	-5463,1
4268,24013	294,50857	27,450603	79,07703	7830,6	540,3114	-6836,9
5423,47118	374,21951	59,251671	23,25624	8335,8	575,1702	-8423,2
5720,94733	394,74537	70,238396	96,12527	8841	610,029	-10237
5456,18145	376,47652	60,399062	27,41074	9346,2	644,8878	-12294
4920,45747	339,51157	43,398915	113,738537	9851,4	679,7466	-14609
6386,99893	440,70293	99,604657	122,5953	10356,6	714,6054	-17198
4758,54922	328,3399	38,978255	131,4037	10861,8	749,4642	-20075
5604,29564	386,6964	65,780835	38,50227	11367	784,323	-23256
6449,7193	445,03063	102,73063	42,01248	11872,2	819,1818	-26756
2883,78628	198,98125	7,6139785	152,8549	12124,8	836,6112	-28631
2135,81045	147,37092	2,8267475	156,9994	12377,4	854,0406	-30591
5699,76347	393,28368	69,414345	98,6587104	12630	871,47	-32638
11401,0278	786,67092	608,8377	100,362911	12882,6	888,8994	-34775

Table A continued

S _y , psi	S _y , Mpa	Poisson's ratio	U _{max,m} Poisson	Young's modulus, GPa	U _{max,m} Young	Vertical displacement, metres	Breakout Pressure Mpa
0	0	0	0,22	0	0	0,016	0
207,44	14,31336	0,49653	0,2746180	1,3347639	2,7285724	0,016	34,43576077
841,1	58,0359	0,48647	0,2735118	3,9828613	0,914417	0,016	125,4198309
1479,56	102,0896	0,47029	0,2717316	4,1666142	0,8740910	0,016	217,115826
2122,82	146,4748	0,45462	0,2700082	4,3615141	0,8350311	0,016	311,3229545
2770,88	191,1907	0,44563	0,2690189	3,4702908	1,0494797	0,016	400,2431564
3423,74	236,2380	0,42785	0,2670640	4,7878762	0,7606712	0,016	491,6205109
4081,4	281,6166	0,42356	0,2665911	4,9772349	0,7317315	0,016	586,4740186
4743,86	327,3263	0,41423	0,2655651	5,8657724	0,6208901	0,016	682,2947651
5411,12	373,3672	0,40595	0,2646546	6,8435593	0,5321792	0,018	769,2929993
6083,18	419,7394	0,38927	0,2628198	6,1102638	0,5960462	0,018	867,381016
6760,04	466,4427	0,38231	0,2620538	6,4274842	0,5666291	0,018	959,908145
7441,7	513,4773	0,38699	0,2625684	10,276438	0,3544029	0,019	1059,599151
8128,16	560,8430	0,38253	0,2620779	11,567311	0,3148527	0,02	1152,721955
8819,42	608,5399	0,36723	0,2603948	7,1252611	0,5111391	0,02	1256,641484
9515,48	656,5681	0,36407	0,2600481	7,5089548	0,4850208	0,02	1339,376849
10216,34	704,9274	0,37457	0,2612031	15,760764	0,2310801	0,02	1434,100916
10922	753,618	0,34626	0,2580884	8,3547711	0,4359185	0,02	1527,836958
11632,46	802,6397	0,34546	0,2580007	21,445755	0,1698238	0,02	1620,520991
12347,72	851,9926	0,3608	0,2596883	9,3186534	0,3908290	0,02	1731,106142
13067,78	901,6768	0,37703	0,2614737	21,7158	0,1677119	0,02	1824,746143
13792,64	951,6921	0,34897	0,2583863	25,206675	0,1444855	0,02	1918,851972
14522,3	1002,038	0,38465	0,2623115	24,664071	0,1476641	0,02	2013,098372
15256,76	1052,716	0,37383	0,2611216	11,678336	0,3118595	0,022	2110,776147
15996,02	1103,725	0,36225	0,2598477	12,375211	0,2942980	0,022	2205,095186
16367,45	1129,354	0,40665	0,2647316	28,182142	0,1292307	0,022	2118,717541
16740,08	1155,065	0,41221	0,2653425	28,854884	0,1262178	0,022	2200,975173
17113,91	1180,859	0,37779	0,2615563	21,819587	0,1669142	0,022	2246,392064
17488,94	1206,73	0,19573	0,2415302	22,810216	0,1596653	0,21	2235,70044

Appendix B

LOG DATA REVIEW OF X-88 WELL

DEPTH PLOT
Scale - 1 : 200

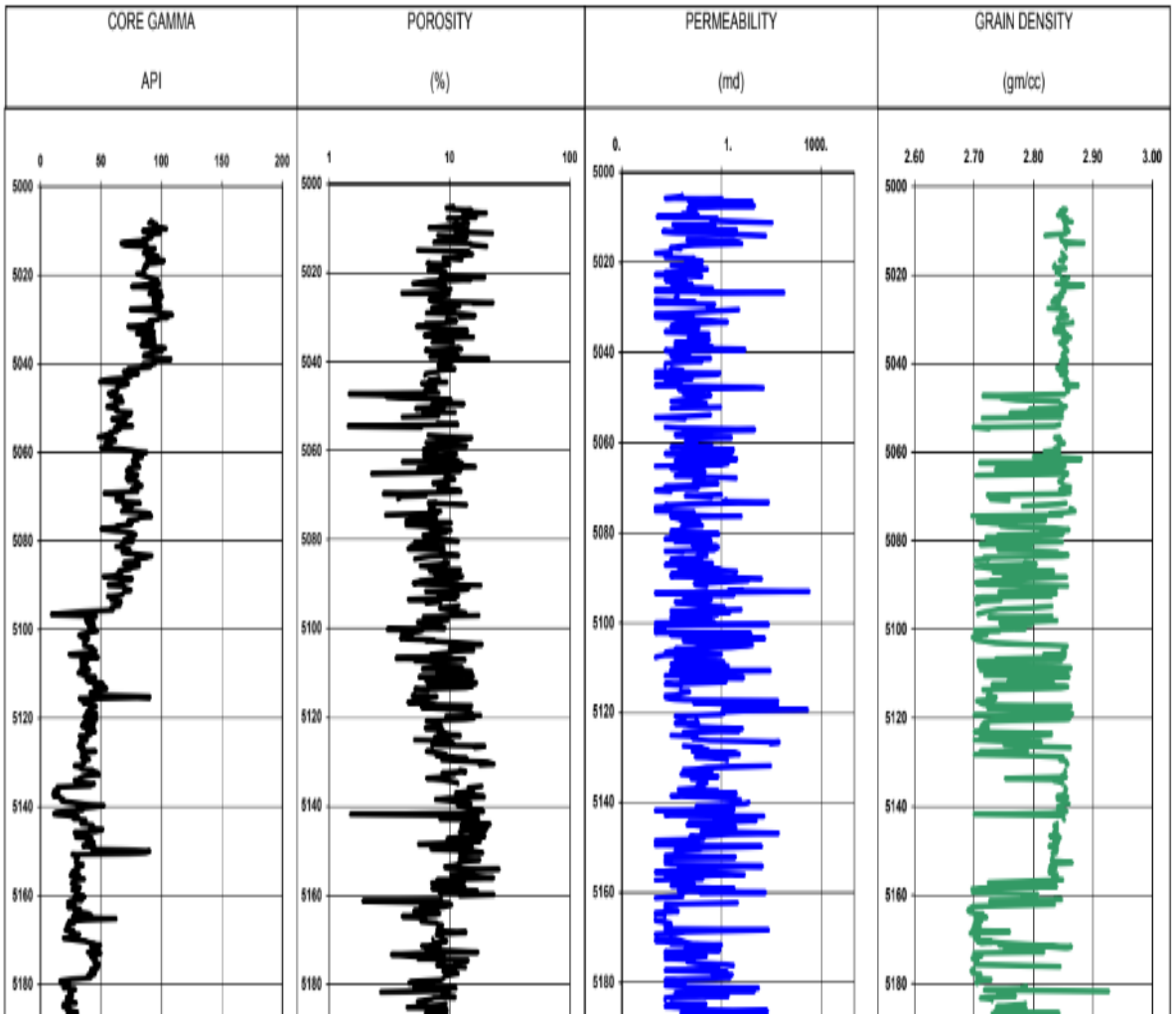


Figure B1. Depth plot on well X-88

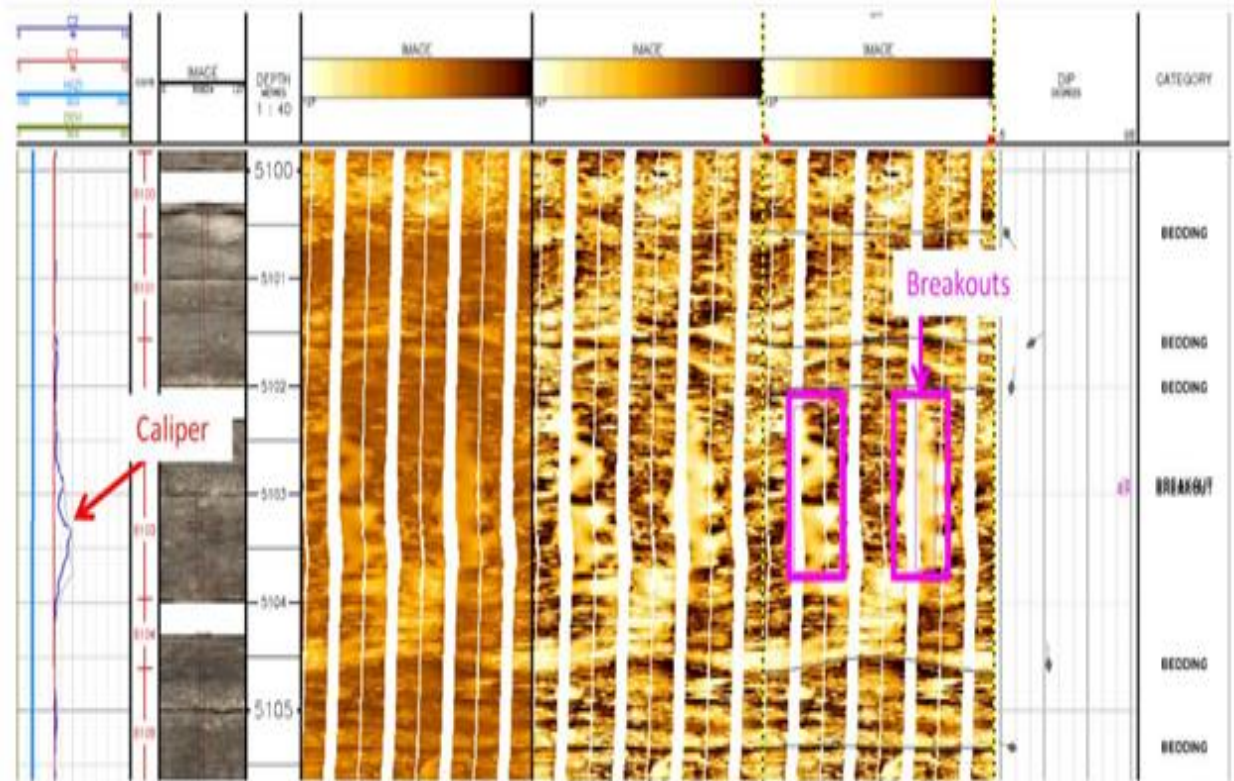


Figure B3. Borehole images showing breakouts are the result of high horizontal stress in the field. The image is from well X-88.